Micromachines for Microchips: Bringing the AFM up to Speed

September 30, 2002
Scientific and Technical Final Report

Sponsored by:
Defense Advanced Research Projects Agency (DoD)
(Controlling DARPA Office)
ARPA Order H927/71

Issued by:
U.S. Army Aviation and Missile Command Under
Contract No. DAAH01-00-C-R218
Contract Effective Date: 18 September 2000
Contract Expiration Date: 18 September 2002

NanoDevices Inc., 5571 Ekwill Street, Santa Barbara, CA 93111
805-696-9002, 805-696-9003 (Fax), steve@nanodevices.com

PI: Stephen C. Minne, Ph.D.

20021023 062

NanoDevices Inc.

REPORT DOCUMENTATION PAGE

Form Approved OMB No. 0704-0188

1. REPORT DATE (DD-MM-YYYY) 30-09-2002	2. REPORT TYPE Final Report	3. DATES COVERED (From - To) Sept 2000 – Sept 2002

4. TITLE AND SUBTITLE
Micromachines for Microchips:
Bringing the AFM up to Speed

5a. CONTRACT NUMBER
DAAH01-00-C-R218

5b. GRANT NUMBER
PAN RTWAX-00

5c. PROGRAM ELEMENT NUMBER

6. AUTHOR(S)
Minne, Stephen, C, Ph.D

5d. PROJECT NUMBER

5e. TASK NUMBER
0001

5f. WORK UNIT NUMBER

7. PERFORMING ORGANIZATION NAME(S) AND ADDRESS(ES)
NanoDevices, Inc
5571 Ekwill Street
Santa Barbara, CA 93111

8. PERFORMING ORGANIZATION REPORT NUMBER

9. SPONSORING / MONITORING AGENCY NAME(S) AND ADDRESS(ES)
Defense Advanced Research
Projects Agency

10. SPONSOR/MONITOR'S ACRONYM(S)
AMSAM-RD-WS-DP-SB

11. SPONSOR/MONITOR'S REPORT NUMBER(S)

12. DISTRIBUTION / AVAILABILITY STATEMENT

Distribution Unlimited

13. SUPPLEMENTARY NOTES

14. ABSTRACT
This Final Phase II SBIR report, developed under contract for topic number DARPA SB992-039, outlines improvements made to the atomic force microscope (AFM) in order to increase its imaging speed 10 to 100 times during standard operation. Faster imaging will allow the AFM to be used in high throughput military and microelectronic manufacturing applications. The developments made under this grant have been commercialized. These products are manufactured and sold in an agreement with Digital Instruments/Veeco. This report outlines the technical achievements made during the entire grant period.

15. SUBJECT TERMS
Atomic Force Microscopy, High Speed Atomic Force Microscopy, AFM, Scanning Probe Microscopy

16. SECURITY CLASSIFICATION OF:

a. REPORT U	b. ABSTRACT U	c. THIS PAGE U

17. LIMITATION OF ABSTRACT
UU

18. NUMBER OF PAGES
46

19a. NAME OF RESPONSIBLE PERSON
Stephen C. Minne

19b. TELEPHONE NUMBER (include area code)
805-696-9002

Standard Form 298 (Rev. 8-98)
Prescribed by ANSI Std. Z39.18

Summary

The scanning speed of imaging in tapping mode with the atomic force microscope (AFM) has been increased by over an order of magnitude. The enhanced operation is achieved by: 1) increasing the instrument's mechanical bandwidth and 2) actively controlling the cantilever's dynamics. The instrument's mechanical bandwidth is increased by an order of magnitude by replacing the piezotube z-axis actuator with an integrated zinc oxide (ZnO) piezoelectric cantilever. The cantilever's dynamics are optimized for high-speed operation by controlling the motion of the cantilever with active feedback. The effect of this control is to reduce the apparent quality factor (Q) of the cantilever. With these two advancements, high speed tapping mode images have been obtained This is the final report for this grant. All grant objectives were completed on time and in budget.

Table of Contents

Introduction

The ever-expanding military demands on the microelectronics, data storage, and biological industries require advancements in technology that are broad-based and crosscutting. Recently, the primary advances in these fields have come through system miniaturization. Advancements through miniaturization have placed a premium on high-resolution surface inspection and imaging. For many applications in these fields, the capabilities of traditional imaging techniques have been stretched to their limits. A robust high-speed high-resolution inspection tool is needed for continued miniaturization and enhanced functionality in these areas.

The atomic force microscope (AFM) was invented in 1986, and has since gained much popularity in high-resolution three-dimensional imaging. A schematic diagram of a typical AFM is shown in Figure 1. The AFM can be used in a wide variety of modes, including fluid imaging, magnetic imaging, capacitive imaging, and thermal imaging. However, the AFM has found its main use in high-resolution surface characterization. The two dominant AFM modes for surface characterization are the contact mode and the intermittent-contact mode.

Figure 1: A schematic of a typical Scanning Probe Microscope (SPM). A image is formed by using the laser/cantilever/detector system to measure the height of every pixel of an image.

In the contact mode, the AFM operates by scanning an atomically sharp tip mounted on soft flexible cantilever across the surface to be imaged. As topographic features on the sample pass under the sharp tip, they cause the flexible cantilever to deflect. A sensor within the microscope monitors the deflection of the cantilever, recording the height of each pixel in the image. Since the raster scan is input by the user, the lateral position can be fed into a computer along with the measured height data, and a three-dimensional image of the surface can be rendered.

Typically, the contact mode AFM is operated in closed loop feedback. The feedback loop monitors the deflection of the cantilever and adjusts the sample position in

4

order to keep the forces between the tip and the sample constant. Maintaining a constant tip sample force preserves the delicate tip and protects fragile samples.

An intermittent contact mode microscope is very similar to the contact mode microscope. For intermittent contact imaging, two additional components are added to the schematic in Figure 1 (not shown). First, a small piezoelectric stack is placed under the cantilever, and second, an RMS to DC converter is placed after the split photodiode. During imaging, the cantilever is oscillated at its resonant frequency by the piezoelectric stack. As the tip rasters over the sample, the topographic data is obtained by measuring the degree to which the sample impedes the cantilever's oscillatory motion through the RMS to DC converter. Like in the contact system, feedback is used to move the sample relative to the tip to maintain a constant tip sample interaction. Otherwise the drivers, the electronics, and the actuators are the same as in the contact mode system. Intermittent contact mode imaging is the preferred method for AFM imaging because it eliminates lateral forces between the tip and the sample. (This mode of imaging is often referred to as Tapping Mode ™, a trade name from Digital Instruments of Santa Barbara, CA.) Elimination of the lateral forces enhances the AFM's image fidelity and preserves the cantilever's tip sharpness.

As features on functional devices continue to shrink, the ability to monitor nanometer scale features "in-line" becomes more important. The AFM has demonstrated its ability to monitor these small features, however its slow speed prevents it from being widely accepted as an "in-line" tool. Currently, AFM images take several minutes to obtain. The speed of imaging depends on the mode of operation, but is generally limited by one of two fundamental parameters. In contact mode feedback imaging, the bandwidth of the feedback loop is the rate limiting parameter. In most AFMs, the speed of the feedback loop is generally limited by the speed of the feedback actuator. In the intermittent contact mode, the feedback loop is still a limiting factor, but no longer the dominant factor. For a typical AFM operating in the intermittent-contact mode, the rate limiting parameter is the speed at which the resonating cantilever can increase its amplitude. This speed is related to the width of the resonant peak, or the cantilever Q. These limitations typically restrict the AFM's imaging bandwidth to 1 kHz in the contact mode and 300 Hz in the intermittent-contact mode.

This research addressed these imaging speed issues by focusing on the fundamental limiting factors of the AFM: 1) the z-axis actuator resonance, and 2) the Q of the oscillating cantilever.

The current z-axis actuator in most AFM systems is typically a bulk piezo-tube about the size of one's finger. Large items typically have very low resonant frequencies, and the typical piezo-tube's first resonance occurs between 600 Hz and 1 kHz. Removing the piezotube from the feedback system can solve this limitation. However the functionality of the actuator is still needed to operate in the feedback mode, so rather than eliminate it completely, in this work it is replaced with a small micromachined actuator integrated onto the cantilever. Because this new actuator is very small it is very fast. The data shows that the micromachined actuator will increase the bandwidth of the AFM by a factor of 100 without losing sensitivity, or total actuator movement.

The width of the resonance of the oscillating cantilever limits the imaging speed because it determines the rate at which energy can be added to (or dissipated from) the cantilever system. For example, if the cantilever has a very high Q (or narrow width),

5

very little mechanical energy can be added per cycle. If the cantilever travels off a step edge, it will take a finite time for the cantilever to "ring" up to its full amplitude. This ring up time determines the free cantilever bandwidth, and has a time constant of Q/w_o. To address this problem, we used a system where the integrated actuator is used to actively damp the oscillations of the cantilever (in addition to adjusting tip/sample spacing).

Phase II Objectives

The overall objective of this Phase II contract was to continue the research and refine the development of an atomic force microscope for high-speed, large-field, imaging in the contact and intermittent-contact modes of operation. The system should be relevant to research, manufacturing, and production applications. In the successful Phase I effort, we developed a proof of concept system based on a cantilever with an integrated piezoelectric actuator and custom electronics. The Phase II effort converted the Phase I designs into commercially viable products.

This project was motivated in part by the SIA roadmap, which explicitly calls out the AFM issues of 1) throughput, 2) tip wear, 3) metrology, and 4) tip aspect ratio. Meeting these industry specific needs will require 1) developing the piezoelectric cantilever into a form suitable for industry and research, as well as increasing its overall throughput potential, and 2) finding the optimal design for the electrical and mechanical subsystems and ensuring that these systems do not degrade the performance of the AFM. These specific objectives are enumerated as follows:

Speed Potential Objectives:
1) Design the ZnO cantilever's resonances to be optimized for tapping mode imaging.
2) Test alternate designs for implementing the frequency dependent filter used in high-speed intermittent contact mode imaging.

Tip/Sample Force Objective:
3) Study the effect of high speed imaging on tip/sample force through a statistical analysis of tip wear.

Resolution Objectives:
4) Design a tall, sharp, high aspect ratio, symmetric tip compatible with the ZnO cantilever fabrication process.
5) Build a final prototype of the optimized ZnO cantilever.
6) Study measurement noise with the high-speed system. If there are any nonfundamental contributions from the high-speed system, redesign as necessary.

Metrology Objective:

7) Study, develop, and refine the system such that it is capable of repeatable metrology using the high-speed cantilever.

Final Objective:

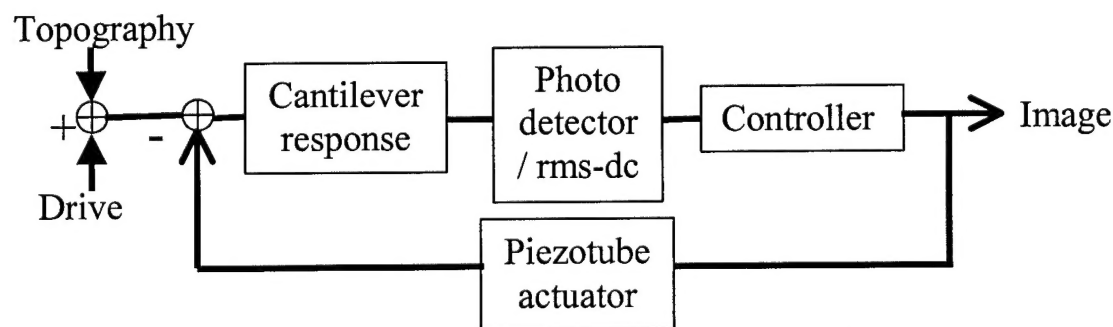8) With above data, prototype a final electronic and mechanical design.

Overall Status and Work Preformed

All objectives and reporting are complete for this contract. The technology developed under this grant has been optimized and fully commercialized. We are currently in a joint development and production agreement with Digital Instruments/Veeco to market the high speed system. NanoDevices and Digital Instruments share in the revenue generated from the hardware sales and NanoDevices sells the consumable high speed cantilever. The product has been widely accepted and has generated much excitement in the scientific community. The technology is included on every new Digital Instruments AFM.

Technical Description

Introduction to Tapping Mode Feedback

In tapping mode, the force with which the cantilever strikes the surface is controlled through the feedback loop. A block diagram of the feedback loop for tapping mode is shown in Figure 1. The cantilever's tapping amplitude is monitored with a photodetector and the ac signal is converted to a dc value. The rms amplitude is compared to a setpoint and the error is used to control the tip-sample height via a z-axis actuator. In this manner, the tapping amplitude is kept fixed. Typically, the z-axis actuator is a piezotube. As the sample is scanned, the piezotube moves up and down in

the z-axis to maintain constant amplitude for the motion of the cantilever.

Figure 1 Tapping mode feedback block diagram.

It is important to maintain a constant tapping amplitude as the tip scans over the surface. Increases in the tapping amplitude can cause damage to the sample as well as premature tip wear.

The setpoint is the value of tapping amplitude the feedback loop is trying to maintain. The setpoint is typically adjusted until the cantilever just touches the surface at the end of its oscillation and thus is slightly smaller than the free air amplitude, a_{free}, of the cantilever. This ensures that the tip is tapping lightly on the sample. A schematic is shown in Figure 2.
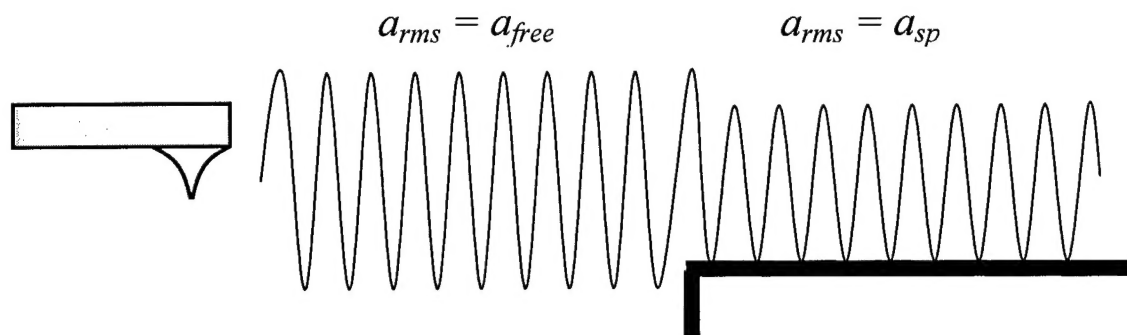
$$a_{rms} = a_{free} \qquad\qquad a_{rms} = a_{sp}$$

Figure 2   The drive produces an oscillation that will reach an amplitude of a_{free}. The sample surface limits the oscillation to the setpoint value of a_{sp}.

The error signal is defined as the setpoint, a_{sp} (the desired tapping amplitude), minus the rms amplitude, a_{rms} (the actual tapping amplitude). The error signal is a measure of how well the feedback loop maintains the desired tapping amplitude. In Figure 3, we show a schematic of the change in a_{rms} caused by a step and the error signal that develops.

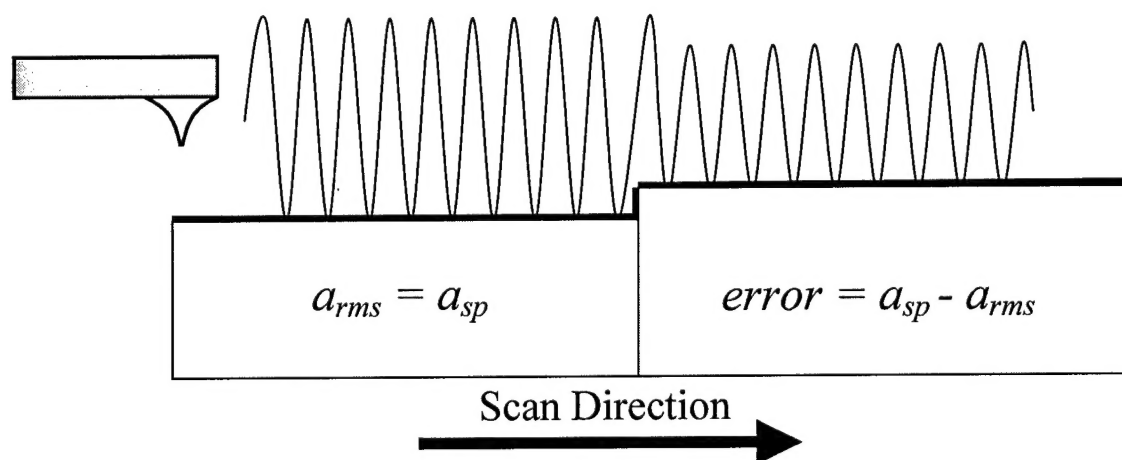$$a_{rms} = a_{sp} \qquad\qquad error = a_{sp} - a_{rms}$$

Scan Direction

Figure 3 Scanning over a step will result in an error from the desired tapping amplitude.

The error signal forms the basis for the feedback signal and is sent to a proportional-integral-differential (PID) controller. This controller generates a signal that

drives the feedback actuator so as to regain the desired tapping amplitude. This signal is a measure of the topography.

While the tapping mode AFM allows nanometer scale resolution with negligible frictional forces, it is encumbered by slow imaging speed. The scan speed of tapping mode AFMs is limited by the speed of the feedback loop that maintains a constant tapping amplitude. For most samples, these constraints limit the tapping mode AFM's scan speed to a few tens of microns per second. At this speed a single, moderately sized 512×512 pixel image will take several minutes to acquire.

The speed of contact mode imaging has been improved by two orders of magnitude solely by increasing the speed of the feedback actuator. However, this scheme does not offer the same benefits for tapping mode. The improvement in scan speed is not strictly proportional to the improvement in actuator speed. In tapping mode, the speed of the feedback actuator is no longer the dominant limiting factor.

Frequency and Time Domain Analysis

It is useful to evaluate the speed limitations of imaging according to two metrics: bandwidth and scanning speed. The bandwidth analysis is illuminating because it is a universal measure that does not depend on surface type. The bandwidth of a system is defined as the maximum frequency at which the output of a system will track an input sinusoid in a satisfactory manner.[1] Higher bandwidth systems allow the cantilever to follow a surface more accurately. Ultimately, one is concerned with scan speed. Scan speed is determined by the bandwidth but also is a strong function of the type of surface imaged. For a given acceptable error signal, flat surfaces allow faster scan speeds while vertical steps require slower scan speeds. Surfaces can be decomposed into spatial frequencies that cover a certain band of frequencies. The maximum scan speed will be determined by those frequencies which lie within the bandwidth of the system. Alternatively, instead of using spatial frequencies, a more direct approach to finding the maximum scan speed may be found with a time domain analysis.

An effective way to evaluate the response of a feedback system is the step response. Vertical steps provide a worst case scenario for the limits on imaging speed. A schematic of the actuator response of a typical system is shown in Figure 4. It can be explained as follows.
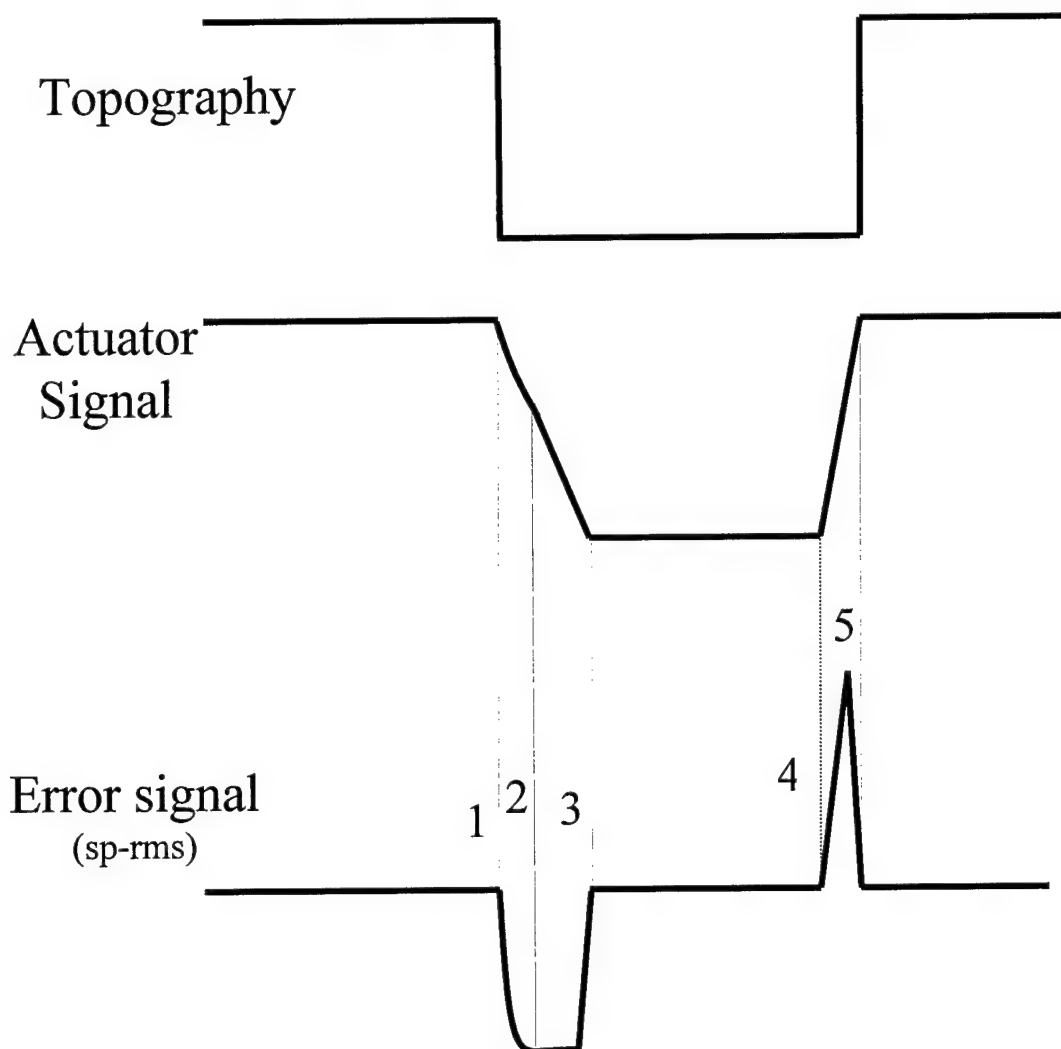
9

Topography

Actuator
Signal

Error signal
(sp-rms)

1 2 3   4

5

1. As the tip scans over the downward step, it is no longer clamped by the sample, allowing the amplitude to "ring-up" according to the cantilever's dynamical response. The amplitude increase will follow an exponential with a time constant on the order of Q/ω_0 where Q is the quality factor of the cantilever and ω_0 is the resonance frequency. Microfabricated cantilevers have inherently high Q, giving typical time constants for transients approaching a millisecond. The inherently **slow transient response**, (see section "2.4" and "2.5" below), limits the growth of the error signal and hence limits the scanning speed if the cantilever is to maintain contact.

2. If the cantilever is scanning fast, the amplitude will reach a maximum, called the free air amplitude, before the actuator can restore the proper tapping amplitude. Here, the magnitude of the error signal will reach a maximum of $(a_{free} - a_{sp})$. The error signal is stalled at a relatively small value (typically 10-20% of a_{free}) until the actuator returns contact with the sample. The problem of a small, maximum error signal is called

error signal saturation, (see section "2.9"), and limits the scanning speed on downward steps. The topography will appear linear, due to the integration in the controller. The slope of the topography signal will be determined by the setpoint and the gains of the PID controller.

3. After feedback restores contact with the sample, the error returns to zero and the topography is once again accurately monitored. The speed with which the actuator can restore accurate topography is determined by the magnitude of the feedback gain. This is limited by the **instability of the high Q system**, (see section "2.6"), as well as the **resonance frequency of the actuator**, (see section "2.7" and "2.8").

4. As the cantilever encounters an upward step the slope in the error signal is steeper than the error signal during a downward step. It is no longer limited by slow transients rather it will be determined by the hard contact between the pyramid shaped tip and the step edge. The magnitude of the error signal is no longer limited to a small value by error signal saturation. It can attain a maximum value less than or equal to a_{sp}—which may be an order of magnitude greater. The larger error signal produces a faster response in the actuator.

5. The tapping amplitude is restored to its desired value and the topography is once again accurately recorded.

In addition, because many systems use analog conversions of the oscillation amplitude to a DC value, there is a trade-off between accurate amplitude measurement and elimination of the carrier signal. For this reason, approximately 10 oscillations are needed for an accurate measure of amplitude. We call this a limit of the **rms to dc converter** (see section "2.10").

Active Damping

The above discussion suggests there are two primary culprits to slow imaging speed in tapping mode operation. The first is the slow z-axis actuator. This has been solved previously. The second involves the dynamics of the cantilever. It will be shown that the high mechanical Q of the cantilever places limits on scan speed which are more severe than the actuator speed limitation. Therefore, the first step to improving speed must address these limits.

If we examine the equation for the motion of the spring, we find that the damping term is proportional to velocity: $F = m\ddot{z} + b\dot{z} + kz$ where m is mass, z is deflection, b is damping factor, k is spring constant, and F is the cantilever drive. The derivatives are with respect to time. The damping factor, b, equals $m\omega_0/Q$. By measuring deflection, and differentiating it, we generate a term that is proportional to the damping term. By feeding this term back to the drive, we can achieve complete control over the cantilever motion such that the damping factor appears to be changed.

This can be implemented in our system as follows. The AFM inherently measures deflection of the cantilever, z. Electronic differentiation converts this measure to velocity, $\dot{z}$. By adding this signal to the drive signal, the equation of motion becomes: $F = m\ddot{z} + (b + D)\dot{z} + kz$, where D is the gain on the differentiation circuit. We call this active damping, and a schematic for the practical implementation is shown in Chapter 3 (Figure 162). The block diagram is shown in Figure 5.
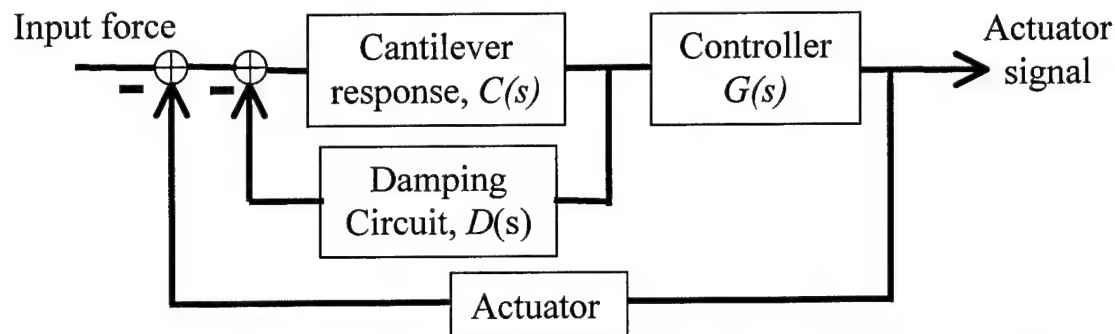
Figure 5   Block diagram to achieve active damping. The canilever response is described by a
                  second order system, the controller is a PID system, and the damping circuit is described
                  by a differentiation.

By adding a term proportional to the damping term we reduce the cantilever's "effective Q" (shown in Chapter 3, Figure 184). It is essential to note that we do not believe that we are changing the cantilever's true Q, as we are not changing the energy stored in the oscillator.[2] If the real Q of the oscillating cantilever were to be changed, it is necessary to change the amount of energy lost to the environment per cycle. This can only be accomplished by changing the aero- or hydrodynamic properties of the cantilever.[3] Rather, we are simply using a feedback loop to reduce the resonances of the cantilever by generating an electrical drive that produces the desired mechanical response. For faster scanning, we want a smaller mechanical response at resonance. Lowering the Q does not , however, change the overall resolution of the system (most tapping mode AFMs are not thermally noise limited), but it will potentially improve imaging dynamics as it changes the response of the cantilever. For simplicity, we will refer to a cantilever without active control as "native" and with active control as "damped."

Other groups have demonstrated control of cantilever spring constant, resonant frequency and Q through optimal control. Mertz et al.[4] and Rugar et al.[5] developed a system for actively damping an AFM cantilever to speed up the system's mechanical transients. Their system used a thermal bimorph actuator to apply the active control. Garbini et al.[6] extended this work by designing a controller for active modification of cantilever dynamics to improve the stability of magnetic force microscopy. Bruland et al.[7] used a similar control system to actively control an ultrasoft magnetic cantilever with an external field. Here, we are implementing active control of the cantilever's effective Q to increase imaging speed by optimizing feedback, not merely to improve transients.

We will now investigate these limits in more detail.

Slow Transient Response of Probe, Bandwidth Analysis

For tapping mode, the cantilever sensor cannot respond to downward steps instantly due to the slow transient response. For a given drive at resonance, high Q systems are limited in the amount of energy that can be added per cycle.[8] The bandwidth for these transients scales as f_0/Q and for typical cantilevers ($Q\sim250$ and $f_0\sim50,000$ Hz) is about 200 Hz. The bandwidth can be experimentally determined by driving the cantilever

at its resonance and modulating the amplitude of the drive. For example, in Figure 6, we monitor the cantilever response while modulating the amplitude of the drive by 100% so that the envelope of the drive has an amplitude that changes from zero to one (in arbitrary units).
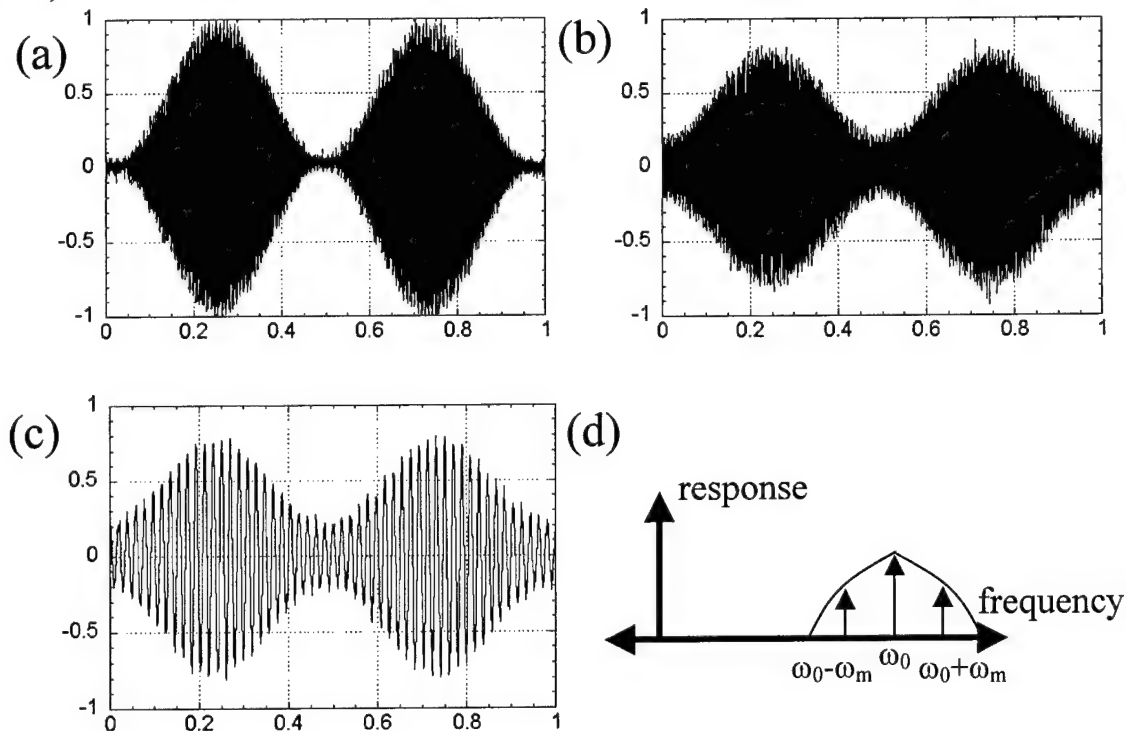

Figure 6   Amplitude modulation of a drive at the resonance frequency. For plots a-c, the x scale is the time for two modulations. The y scale is in units of full amplitude response. d) shows a schematic of the spectrum response for an amplitude modulated cantilever.

In Figure 6a, the modulation frequency of 10 Hz is slow enough such that the cantilever response follows the drive perfectly, with a response that also changes from zero to one. As the modulation frequency is increased, the response of the cantilever becomes immune to the modulation envelope due to the slow transient response. Eventually, the amplitude of the envelope for the response of the cantilever is reduced to 0 for high modulation frequencies. We define the bandwidth of the transient response as those modulation frequencies where cantilever has a significant response (a 3 dB reduction or less). This is schematically shown in Figure 6d where the spectrum response of a harmonically driven, amplitude modulated cantilever is given. In Figures 2.6b and 2.6c, we show the response to 100% modulation of the drive for the native cantilever and a damped cantilever for higher modulation frequencies. For both cantilevers, the response envelope is reduced by 3 dB of the input envelope. For a native cantilever this bandwidth is 2*120 Hz (Figure 6b). Additional damping of the cantilever by close proximity to the surface, known as squeeze film damping,[9] reduces the native Q by a factor of 3 or more while imaging (so typical values while imaging are about 75). This increases the bandwidth limit to approximately 2*400 Hz. Controlling the dynamics of the cantilever through active damping allows us to increase the speed of the transient response to the point where the limit of the rms to dc converter is approached (roughly 10 cycles must be

13

recorded to convert an ac signal to a dc value). In Figure 6c, we show an actively damped cantilever where the bandwidth limit due to transients can be increased to over 2*2 kHz, by reducing the effective Q by a factor of 15.

Slow Transient Response of Probe, Scan Speed Analysis

For accurate imaging the topography signal should be proportional to the change in topography – unfortunately, this is not always true. The tip can lose contact with the surface as is evident from Figure 4 where the amplitude reaches its free air amplitude before event two. To maintain contact between the tip and surface, the scanning speed must be reduced.

The scanning speed limit due to transient response is dependent upon the type of surface imaged as well as the damping of the cantilever. The scan speed limit due to slow transients can be analyzed as follows. If the sample contains a sharp downward step, the sample will no longer clamp the oscillation at a_{sp}, and the driven cantilever's amplitude will increase and saturate at the free air amplitude, a_{free}, as shown in Figure 7.
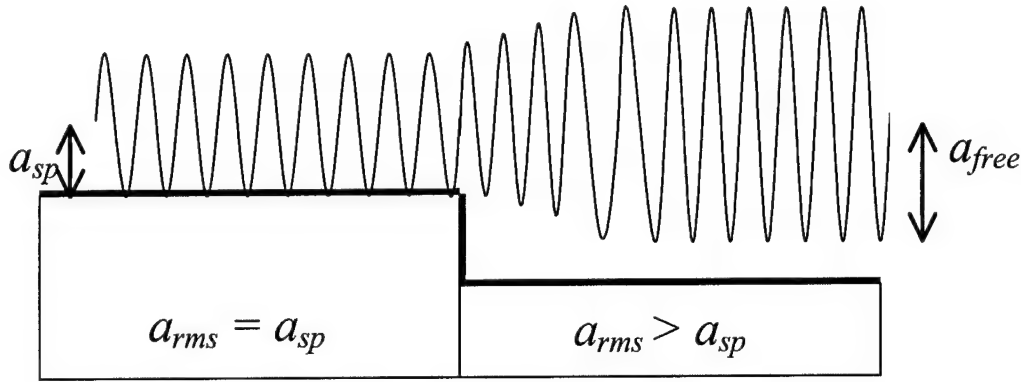

Figure 7 Schematic showing the amplitude ring-up as the tip scans over a downward step.

The amplitude increase as a function of time is given by:
$$\Delta a(t) = \left[a_{free} - a_{sp}\right]\left[1 - \exp\left(-\omega_0 t/2Q\right)\right]. \tag{1}$$
For a standard cantilever imaging a surface in air, viscous and squeeze film damping produce a Q of approximately 75. Taking ω_0=300,000 radians/s, a free air amplitude of 50 nm, and a setpoint of 80% of the free air amplitude, the amplitude increases initially at 4 Å per cycle.

For the cantilever tip to remain in contact with the surface at each cycle, the tapping amplitude must increase faster than the surface drops away over the downward step. The surface drops away according to the convolution of the tip with the step edge. The convolution of the spherical tip and the step edge will be spherical. In Figure 8a we show this schematically where R is the tip radius of curvature, v is the scan velocity, and T is the period of the oscillation. Here the tip radius of curvature is 10 nm and the period is 0.02 ms. To maintain contact every cycle, vT must be less than the difference of the squares of the other two sides of the triangle shown.
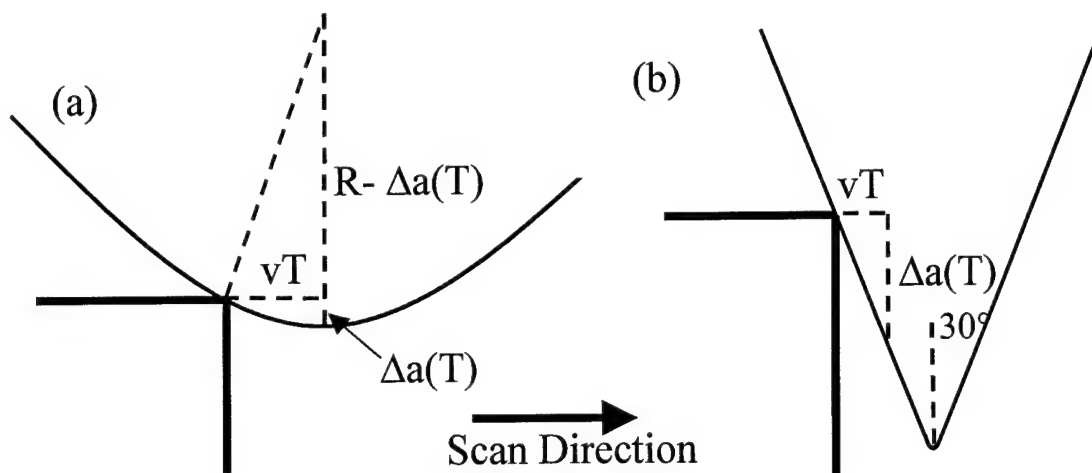
14

Figure 8   Schematic showing the convolution of a step with the a) spherical tip or the b) cone of the tip.

The scan rate must be less than:

$$v = \sqrt{R^2 - (R - \Delta a(T))^2}\big/T,$$ (2)

or 140 µm/s. Scans faster than this will not maintain contact with the surface with each oscillation, resulting in poor topography representation.

The problem of slow transients is more pronounced when the tip scans past the edge where the cone of the tip rather than the apex is in contact with the edge. The cone angle on silicon tips is approximately 30 degrees. As shown in Figure 8b, to maintain contact with the surface after every oscillation, the scan velocity must be less than:

$$v = \Delta a(T)\tan(30)/T,$$ (3)

or 12 µm/s.

Increasing the tapping amplitude and maintaining the same 80% setpoint increases both $\Delta a(T)$ and the scan speed. Scan speed can also be increased by using a cantilever with a higher resonance frequency (for a given Q). The amplitude will increase the same amount every cycle but each cycle takes less time, resulting in a faster possible scan speed. Resonance frequencies of 200 kHz, or more, are commonly used, increasing this limit by a factor of 4 or more. Operating on a higher resonance can likewise increase scan speed.

Alternatively, $\Delta a(T)$ can be increased with active control. Decreasing the effective Q of the cantilever increases the amplitude gain per oscillation. The effective Q can be reduced to 15 or below, producing $\Delta a(T)$ of 1.8 nm per cycle for the same 40 nm tapping amplitude (setpoint). The velocity limit is now 286 µm/s while the spherical tip is in contact with the step and 52 µm/s when the tip cone is in contact.

Instability Due to High Cantilever Q

When imaging, we desire a large feedback gain while maintaining stability. Higher gain improves the response of feedback and results in smaller errors. Yet, high gain pushes the system towards instability. For stable feedback, the gain of the loop should be small for the frequencies where the signal from the controller and the response

of the actuator are out of phase. Otherwise, the controller sends a signal to the actuator to move one way, but in reality it is moving the opposite. The error is amplified over and over as it travels around the loop, causing an instability and loss of control. Instability places an upper limit on the open loop feedback gain and in turn limits the imaging speed.

For the cantilever system, the 180 degree phase shift occurs for frequencies above ω_0. At ω_0, the closed loop gain must be less than one. For a given error, the loop gain is proportional to the feedback gain, G and the cantilever-actuator system response C, as shown schematically in Figure 9. C is described by a second order system while G is described by a PID system.
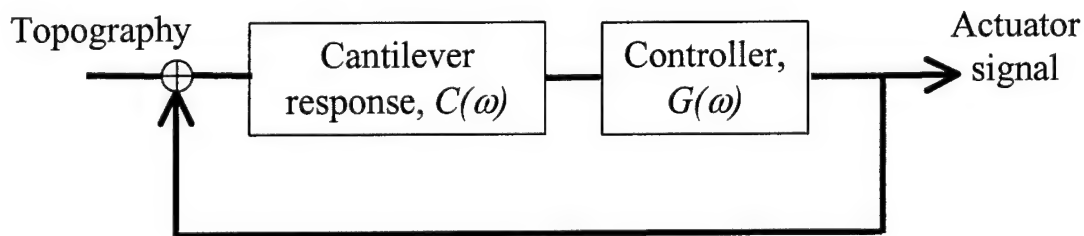

Figure 9 Block diagram of the closed loop showing the cantilever response and the controller.

The product $G*C(\omega = \omega_0)$ must therefore be small enough to ensure a closed loop gain less than one. $C(\omega_0)$ is proportional to the cantilever Q. Thus, by decreasing the effective Q, G can be increased proportionally. Through active control, the effective Q can often be reduced by a factor of 5 or more, allowing an increase of feedback gains and a decrease in the error signal by a similar amount.

This is demonstrated in Figure 10. In (a), we show the topography, error signal and phase of a scan of a silicon grating. In the second set of traces, (b), the cantilever has been actively damped such that the feedback gain is increased by a factor of 4, reducing the error signal by a like amount. If one is willing to accept the original error signal, then the scanning speed can be increased proportionally, as shown in the third set of traces, (c).
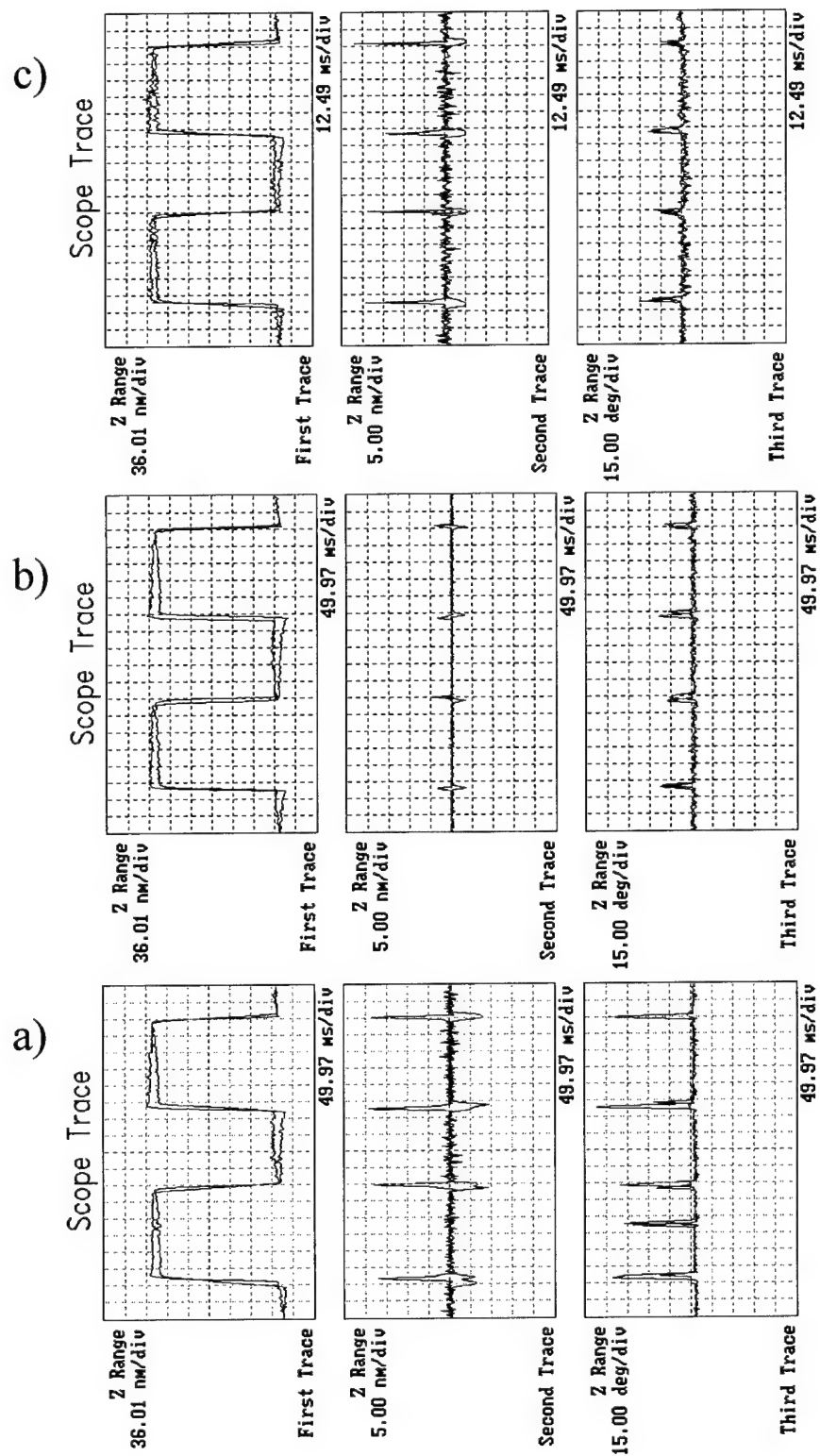
Figure 10   Line traces showing topography, error, and phase for a) native cantilever, b) damped cantilever, and c) damped cantilever at four times the speed.

Feedback Actuator Speed, Bandwidth Analysis

The bandwidth for linear response of the actuator is limited by its resonance frequency. In addition, the high Q of the resonance provides a problem for the stability of the system – the imaging bandwidth of the feedback actuator should be determined from the closed loop transfer function. As the frequency of the input increases, the response of the actuator begins to lag the input. When the lag becomes large, the system becomes unstable. The measure of bandwidth that is often used is a phase margin of 45 degrees in the closed loop. This phase margin indicates the frequency at which the phase lag between the input and response of the system reaches 45 degrees. Using these criteria, the piezotube is limited at 1.5 kHz, while the ZnO integrated actuator is limited at 45 kHz, as shown in Figure 11.
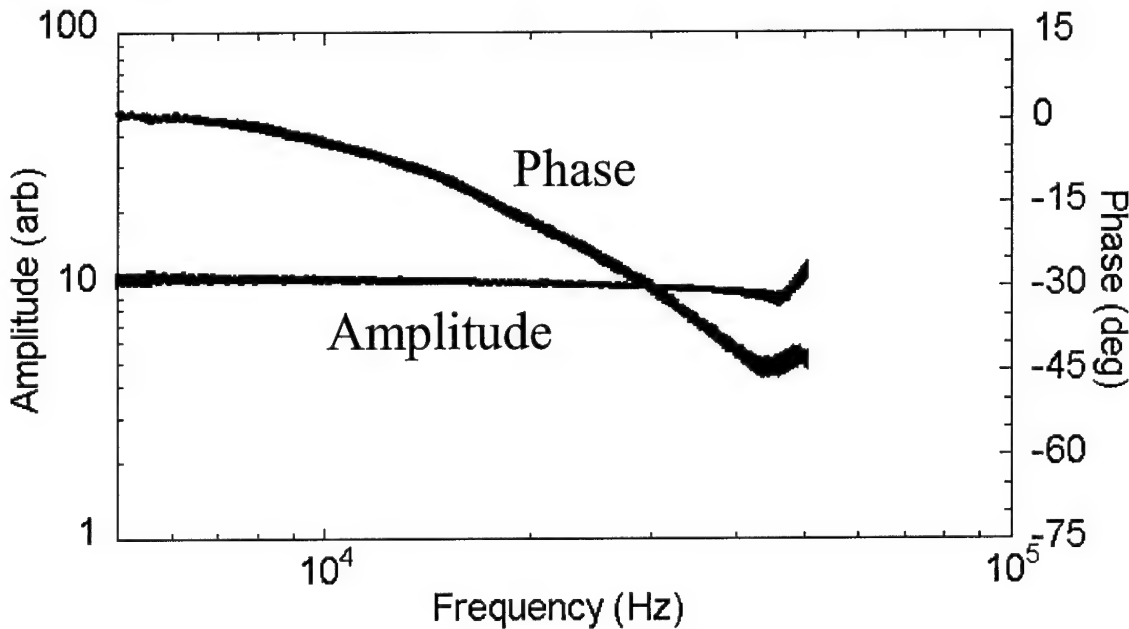

Figure 11   Closed loop transfer function of the ZnO actuator.

Feedback Actuator Speed, Upward Step Scan Analysis

For upward scans, a higher resonance frequency translates into an increase of imaging bandwidth. In the time domain, a higher resonance frequency allows a faster response time to applied forces. The speed of imaging is limited by the time the actuator can restore a zero error signal; a higher resonance frequency translates directly to faster imaging.

The magnitude of response of the actuator is determined by the magnitude of the error signal and the feedback gain of the controller. Because the resonance of the actuator contains a 180 degree phase shift, it is important that the closed loop gain is kept less than one at or above resonance. To maintain a small steady state error, a large gain is desired. The controller is dominated by the integrator and the gain of the integrator rolls off at 20 dB per decade of frequency increase. This allows for a large gain at low frequencies and a smaller gain at the resonance. The actuator signal, $z_{actuator}$, scales as:

$$z_{actuator} = G_i \int error(t)dt, \tag{4}$$

18

where G_i is the gain on the integrator. Increasing the resonance frequency allows an increase in G_i by 20 dB for every decade increase of ω_0. Increasing G_i directly results in a proportional increase in scan speed.

As the cantilever scans over an upward step, the amplitude is sharply reduced as the surface clamps the oscillation of the cantilever. For steps larger than the tapping amplitude, oscillation can be completely quenched, in which case the error signal becomes saturated at a_{sp}. Not only does this cause increased vertical force, but with the tip now in continuous contact, the shear force is likely to damage both the sample as well as the tip. To avoid this, the error signal must always remain less than the setpoint.

For fast scans, it is possible to quench oscillation after one cycle. For a vertical step, we must consider the convolution of the tip and sample, which is dominated by the cone angle of the tip. A glance at Figure 8b will show that a scan of distance vT towards the step, where T is the period of oscillation, will clamp the oscillation by $vT\tan(30)$. Therefore, a velocity of:

$$v = a_{sp} \tan(30)/T,\tag{5}$$

will quench oscillation in one cycle or about 1154 µm/s.

For slower speeds, oscillation can also be quenched over more than one cycle if the amplitude decrease from surface clamping is faster than the actuator can increase the tip sample distance. For example, if every cycle, the amplitude is reduced by 5 nm, then in 8 cycles, the amplitude will be reduced to zero.

Although the response of the system with a complex error signal can be difficult to determine analytically, we may simplify the system with several assumptions. Clamping in the z direction over duration Δt is described by $v\Delta t/\tan 30$ where Δt can be taken to be small when compared to the response time of the actuator. The actuator signal will then take the form of a step response, with a step height determined by magnitude of the error signal. Therefore, the scan is limited by the time it takes for the feedback to respond to this error signal. The actuator's response can be simulated as a second order system in closed loop with a PID controller.[10] We model the system as shown in Figure 5.

In Figure 12 we show the unit step response of the system for the piezotube and integrated actuator. For a system dominated by an integrator, the response approximates a linear function of t for a unit input. The slope of the actuator's unit step, c, is determined by the rise time from 10% to 90% response. Using the 10% to 90% rise time, the value of c is ~550 s^{-1} where the feedback actuator is a piezotube, to ~1250 s^{-1} for the ZnO actuator. The damped cantilever with ZnO actuator allows larger feedback gains with a c of ~10,000 s^{-1}. With these values, the response to the step input occurs in 1.8 ms, 0.8 ms, and 0.1 ms respectively.
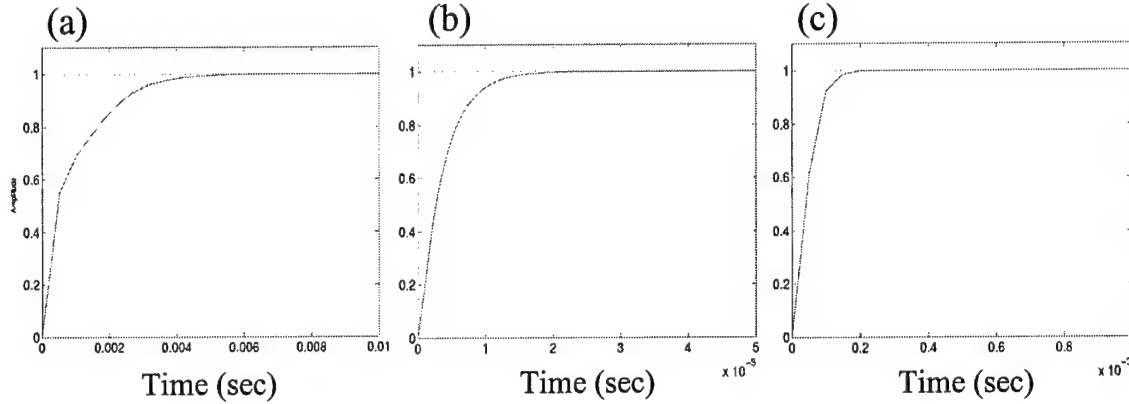
Figure 12   Step response of the control system for the a) piezotube, b) ZnO, and the c) damped ZnO.

The error as a function of t can be defined as the difference between the clamping of the cantilever's amplitude by the step and the response of the actuator to compensate for this step. This is shown schematically in Figure 13.
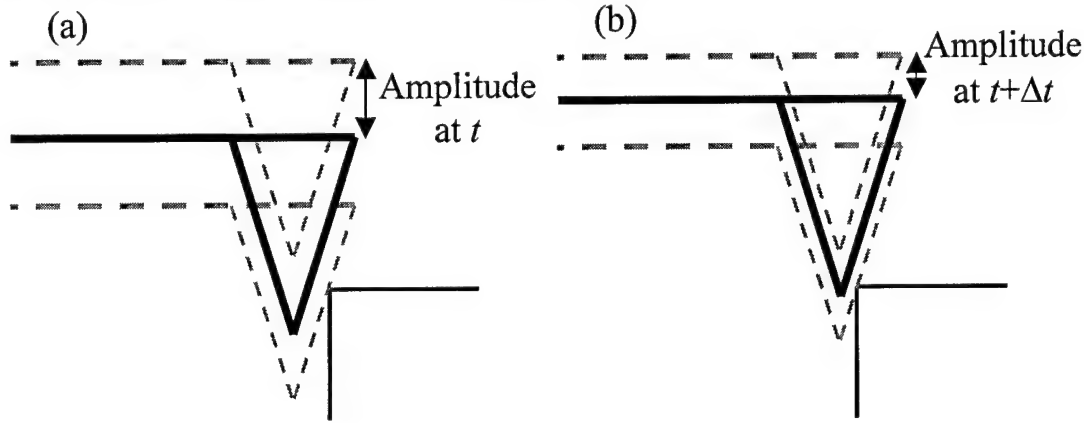

Figure 13   Cantilever clamping due to a step up. The solid schematic represents the center position of the oscillating cantilever, while the dashed lines represent the maximum extent of oscillation.

A cantilever at time t will have a given tapping amplitude. As the tip scans into the step, the amplitude will be reduced. However, the actuator will seek to increase the distance between the tip and sample. Analytically, the error signal can be determined by dividing the time into smaller units of Δt, which are small compared to the response time of the actuator. The incremental increase in the error signal over a unit of time is given by the surface clamping over that time minus the movement of the actuator over that time:

$$error(t + \Delta t) - error(t) = z_{clamping}(\Delta t) - z_{actuator}(\Delta t). \tag{6}$$

As the tip scans over the upward step, the vertical clamping of the surface per unit time scales like $v\Delta t/\tan 30$. For small Δt, the response of the actuator for a given input is the unit step response, $c\Delta t$, times the magnitude of the input, $error(t)$, or $z_{actuator} = error(t)c\Delta t$.

We can analyze the error signal as a function of t by dividing the time into small units of Δt with $t_n = n\Delta t$, where n is an integer increasing from zero. Thus, t_0 represents the time at which the tip first comes in contact with the step, t_1 equals $t_0 + \Delta t$ and so on. Then:

20

$$error(t_n) = error(t_{n-1}) + v\Delta t / \tan 30 - error(t_{n-1})c\Delta t. \tag{7}$$

For example, taking Δt to be the time for one oscillation (about 0.02 ms), $error(t_0)$ is zero. The error for one oscillation later is $error(t_1) = v\Delta t/\tan30$ (there is not yet an actuator response). However, by t_2 the actuator responds with $vc\Delta t^2/\tan30$ and so:

$$error(t_2) = \frac{v\Delta t}{\tan 30}(2 - c\Delta t), \text{ and} \tag{8}$$

$$error(t_3) = \frac{v\Delta t}{\tan 30}(3 - 3c\Delta t + c^2\Delta t^2). \tag{9}$$

Surface clamping will continue during the time that the tip is in contact with the step. For a step of height H, the tip is in contact for all $t \leq H\tan 30/v$. We define $n' = \dfrac{H\tan 30}{v\Delta t}$ to be the time at which the tip passes the step. By induction,[11] the error as a function of t_n is:

$$error(t_n) = \frac{v\Delta t}{\tan 30}\sum_{b=0}^{n-1}(-c\Delta t)^b\frac{1}{(b+1)!}\frac{n!}{(n-b-1)!}, \tag{10}$$

for all $n \leq n'$. After this time, clamping no longer occurs and the error signal will steadily decrease by a factor of $(1-c\Delta t)$ every Δt unit of time. For all $n > n'$, the error is:

$$error(t_n) = error(t_{n'})(1 - c\Delta t)^{n-n'}. \tag{11}$$

The duration of Δt is small compared to the time of response, therefore the initial slope of the step response is the most appropriate measure of the c parameter. In this case, c has values of 1250 s^{-1}, 3300 s^{-1}, and 14300 s^{-1} for the piezotube, ZnO, and damped ZnO actuators respectively. The above equation can be numerically solved and the error is found to increase to a maximum value determined by the scan speed and the speed of the actuator. If we encounter a step height of 200 nm and set a limit to the maximum error that attained for downward steps (10 nm for a 40 nm setpoint and 50 nm free air amplitude), then scan speeds are limited to 10, 29, and 116 μm/s respectively.

Figure 10 shows a typical scan line trace of a 200 nm step. In all cases, the piezotube is used as the feedback actuator with its topography signal shown in the first trace for each set. The second trace in each set shows the error signal. The positive spikes indicate an rms amplitude smaller than the desired amplitude while scanning over an upward step. For the scan velocity of 20,000 nm/s and a step height of 200 nm, the tip is in contact with the step edge until time $n=285$. The plot of the error as a function of n, as calculated from the above equation, is shown in Figures 2.14a-c. For the case of the piezotube actuator, (Fig. 2.14a), the maximum calculated error signal is 28 nm. The root mean square of the calculated error signal gives approximately 20 nm, and this compares well with the observed value (Fig. 2.10a). After this maximum, the error signal decreases and becomes negligible at a final time $n=500$, or $t=10$ ms. This again compares well with the measured time of spike of 15 ms from Figure 10a. In Figure 14b, we show the calculated error as a function of n when a piezotube actuator is used in conjunction with a damped cantilever. The damped cantilever allows us to increase the feedback gain which reduces the error of the step response. The maximum error is calculated to be 7 nm (5 nm

21

rms), which again is close to the error shown in Figure 10b. The calculated error signal for the damped ZnO actuator is shown in Figure 14c. Finally, Figure 14d shows data from a scan so as to compare with the calculation. Here, the error signal is monitored during an upward step. The tip makes contact with the step at approximately $n=250$ and the error increases to a magnitude of 25 nm. The observed shape is similar to what is calculated. The small peaks in the error are due to the imperfections on the tip and step edge. This trace is an average of 16 scans.
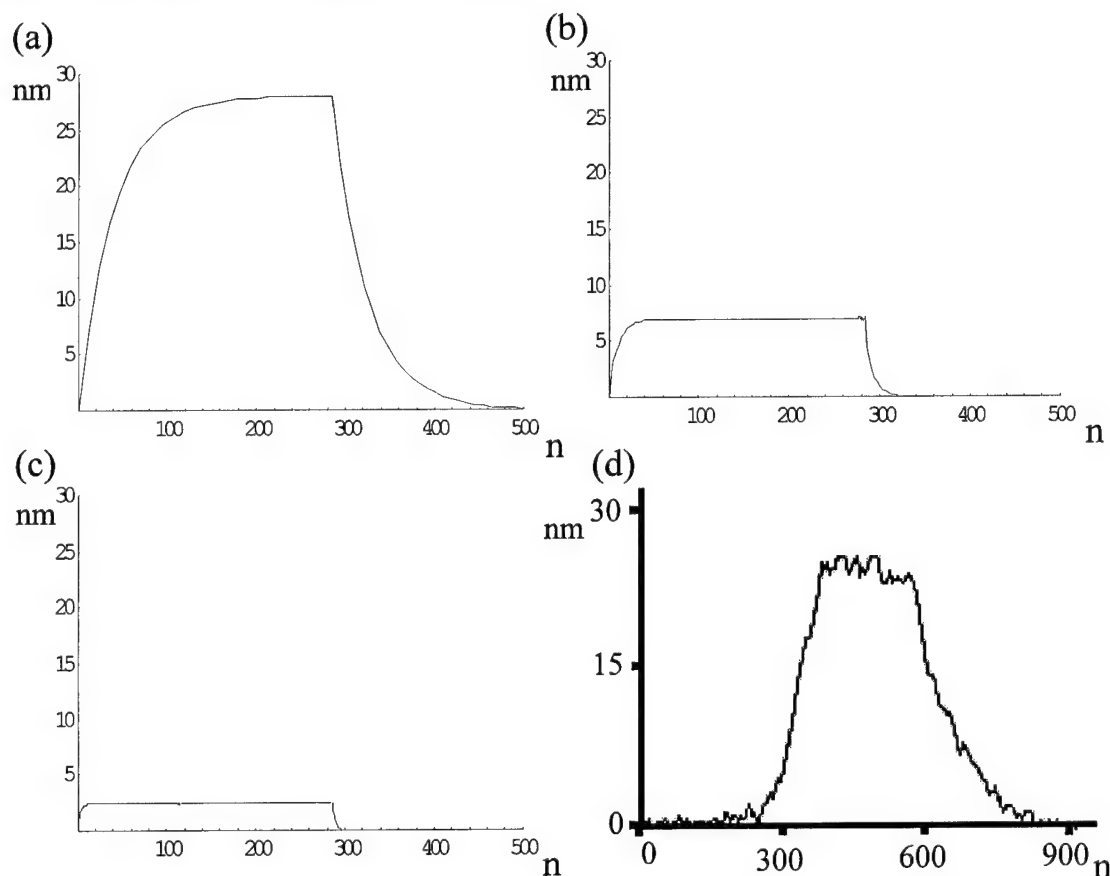

Figure 14   Simulated error signal while scanning over a 200 nm step for the a) piezotube, b) ZnO, and the c) damped ZnO actuators. d) is data showing the error signal for the piezotube actuator.

Error Signal Saturation

Since the setpoint is chosen to be close to the free air amplitude, the maximum error signal on a downward step is small. As the error signal determines the actuator signal (after integration), a limited error signal constrains the feedback loop to a relatively slow response. This limitation is called "error signal saturation." Typically, the setpoint is chosen to be as close to the free air amplitude as possible. Therefore, the maximum magnitude of the error signal for downward steps is $a_{free}-a_{sp}$. This is typically under 20% of the free air amplitude. The speed of tapping mode imaging can be increased by simply using a smaller setpoint, since this allows a larger error signal while scanning over

22

downward steps. However, this strategy requires a stronger tapping force, which is undesirable.[12]

With the description presented in a previous section, the unit step response of the actuator for a closed loop system follows $z_{actuator}=error(t)ct$ where c=550, 1400, 10000 s^{-1} for the piezotube, ZnO, and damped ZnO actuators respectively. For a downward step larger than a few nanometers, the time to negotiate the step will be larger than the millisecond the amplitude takes to respond. The magnitude of the error signal will saturate at $a_{free}-a_{sp}$, or approximately 10nm for a setpoint of 40 nm. The actuator signal due to a downward step is then: $z_{actuator}=(a_{free}-a_{sp})ct$ or $z_{actuator}=10ct$, where $z_{actuator}$ is in nm. For a downward step of H nm, the limited error signal requires $t=H/10c$ to move the actuator H nm (note c has units [sec]$^{-1}$ and 10 has units [nm]). In that time, the scan covers Htan30 nm. The scan velocity is limited to:

$$v = 10cH\tan 30 / H \text{, or} \tag{12}$$
$$v = 10c\tan 30. \tag{13}$$

The scan speeds to maintain contact with the step at all times after ring-up are limited to 3.2 μm/s, 8 μm/s, and 58 μm/s respectively. Most operators do not require constant contact with the surface over downward steps. Typically, this does not increase tip wear or sample damage, because the tip is not in contact with the surface during this time. For example, the scan over a downward step in Figure 10a has a negative error signal that is stalled at about -10 nm (corresponding to an increase of a_{rms} from a_{sp} to a_{free}), The tip loses contact with the surface for over 35 ms on the downward step, during this time the tip scans 0.7 μm, or about 3.5 % of the scan. The setpoint and tapping amplitude are chosen such that the maximum error signal for downward steps is about 10 nm. During the 35 ms that the tip and sample are out of contact, the piezotube actuator is moving down to follow the step. Moving $10ct$ nm for the time out of contact, the actuator moves 200 nm, equal to the step height, to regain the zero error signal.

RMS to DC Converter

Most commercial systems use analog techniques to demodulate the tapping amplitude into a dc measure. This is typically done with an rms to dc converter. The rms to dc converter measures the true rms amplitude of the oscillating cantilever, where the instantaneous position of the cantilever is measured by the photodetector and the averaging time is set by the time constant on the chip. Typically, the time constant is equal to the time needed for 10 oscillations. This time constant ensures the carrier frequency does not leak through significantly in the signal. If the resonance of the cantilever is 50 kHz, the bandwidth is then limited to 5 kHz. This can be increased by using the second resonance of the cantilever[13] or by fabricating smaller cantilevers with higher resonance frequencies.[14] The scan speed for the tapping mode images in Chapter 3 (Figure 228) are constrained by this limitation.

Review of Scan Speed Limits

Many of the limitations described here are interrelated and cannot be easily isolated to determine the greatest limitation on scan speed. For example, although the limits due to slow transients are not typically as severe as that of error signal run out, the slow transients introduce time delays, which has an effect on the stability of the system, and hence requires reduced gains. In addition, many specific parameters will vary from

system to system and should be taken into account. For example, resonance frequency, setpoint, and tapping amplitude all have significant effects on scan speed.

With this in mind, we list the limits of bandwidth and imaging speed for conventional tapping mode imaging with a piezotube actuator in the following chart. The imaging speed limits were determined by examining the response of the system to upward and downward steps in topography. In addition, we list the improvements that can be had by using the faster, integrated actuator and utilizing the instrumentational advances of active control and operating on a higher resonance.

Table 2.1 Scan speed limits

	Conventional Limit	Improved limit
Slow transient response	800 Hz / 12 μm/s	2000 Hz / 52 μm/s
Actuator response	1000 Hz / 10 μm/s	40 kHz / 116 μm/s
error saturation	3 μm/s	58 μm/s
rms to dc converter	5 kHz	15 kHz

These calculations are based upon ideal steps in surfaces. In practice, there are no perfectly vertical steps, which is to our advantage. The limits described here are thus tempered by this fact. In addition, significant leeway can be had by the operator. If the sample is particularly robust, then discretion can be used when deciding upon the setpoint or the acceptable error signal.

For an AFM operating in contact mode, where the tip is in continuous contact with the microscope, the scan speed can be significantly faster than tapping mode. In contact mode, the cantilever is heavily damped by the surface. Therefore, the problem of high Q systems are not a limitation to speed. Moreover, the problem of error signal saturation is avoided because of the strong attractive force that exists between the tip and sample due to capillary forces. We conclude that inertia plays a larger part in limiting the scan speed.[15]

Motivations for High Speed Tapping Mode

For most samples, the tapping mode AFM's scan speed is limited to a few tens of microns per second. At this speed a single, moderately sized 512 × 512 pixel image will take several minutes to acquire. Since the AFM platform can provide nanometer resolution for a variety of surface characterization and modification objectives, including lithography,[16] data storage,[17] chemical mapping,[18] and DNA fingerprinting,[19] it is important to increase the scanning speed to further enable these applications.

For example, reducing the acquisition time for the image has important ramifications for biological and clinical applications. Determining the length of DNA strands is an ideal application of a high resolution AFM. Accurate determination of DNA lengths, or "sizing," is important for applications such as foot-printing (finding out where enzymes stick), restriction mapping (determining where a DNA strand is cut), plus/minus screening (determining if a gene is expressed), and genotyping (finding out which genes are present). Currently, the method for determining the size of DNA strands centers on gel electrophoreses. Sample DNA is extracted and amplified using polymer chain reaction (PCR)[20] to generate significant quantities of DNA for use in the gel. The process of PCR uses cellular machinery to make copies of a given strand. To produce the

quantities needed for sizing by gels, often 30 cycles or more are necessary, increasing time and probability of error. In addition, the gels may take 1 to 2 hours to separate.

A method for sizing DNA using the AFM as an analytical tool has been developed in Jan Hoh's laboratory.[21] The method involves adsorbing strands of DNA onto a mica substrate. The AFM images the adsorbed DNA, thereby determining its size. Hoh has found that the technique can be used to distinguish a 200 base pair (bp) fragment from a 250 bp fragment. The high SNR of the AFM makes it possible for single molecule sensitivity in DNA sizing experiments, decreasing the number of PCR amplification steps. The application is important where speed is critical, such as evaluations of pathological samples during diagnosis.

The AFM technique suffers from two drawbacks. One is the slow scanning speed of imaging. The second is the limited scan area. Although a five minute image is significantly faster than a one hour gel, obtaining high resolution images may require several large scale scans to find the strands and then zooming in to provide the necessary detail. Moreover, finding DNA on the surface will be difficult if the sample density is low; a goal that is desired to reduce the number of PCR steps. The ultimate goal is the detection of a single 100 nm long strand of DNA on a 1 cm^2 surface. This goal cannot be achieved with the current scan size of 10^{-4} cm^2 for a single cantilever in commercial systems. High-speed imaging with real-time visual feedback and parallel arrays would make finding small numbers of molecules more feasible.

In addition, the AFM may provide solutions to clinical problems previously unsolved. Woolley et al., have developed a method for direct haplotyping of kilobase-size DNA through AFM imaging.[22] Haplotypes refer to variations at a specific gene site on a DNA strand that can indicate a predisposition to a genetic disease. Traditional gene sequencing techniques are ill equipped to address on which of the two copies of a chromosome the change resides. If one chromosome contains the defect, there is no way to tell on which chromosome the errant base pair resides. At best, family studies can be used to investigate.

The authors used a probe with a single-walled carbon nanotube tip to image a labeled DNA strand at high resolution. Oligonucleotides labeled with larger molecules are hybridized specifically to complementary target sequences in template DNA, and the positions of these larger molecules are determined by direct imaging. The approach permits haplotype determination from simple visual inspection of AFM images of individual DNA molecules.

Other Approaches For High Speed Tapping Mode in Air

Approaches for high speed tapping mode imaging in air have do so at the cost of tip-sample force. Ookubo et. al.[23] obtained a 225 μm/s speed by combining the feedback signal and the error signal into a composite topographic signal. This implies the feedback is not maintaining a small error signal, which increases force on soft samples.

Effect of Active Damping on Resonance and Transients

We have increased the tapping mode imaging rate with two improvements. First, a faster z-axis actuator is integrated onto the cantilever. Here, we use a ZnO piezoelectric actuator to both drive the cantilever at its resonant frequency and to provide z actuation.

Second, an active damping circuit is applied to increase the speed at which the control loop can respond.

The damping circuit is accomplished with a feedback loop in the drive circuit, as shown in Figure 1.
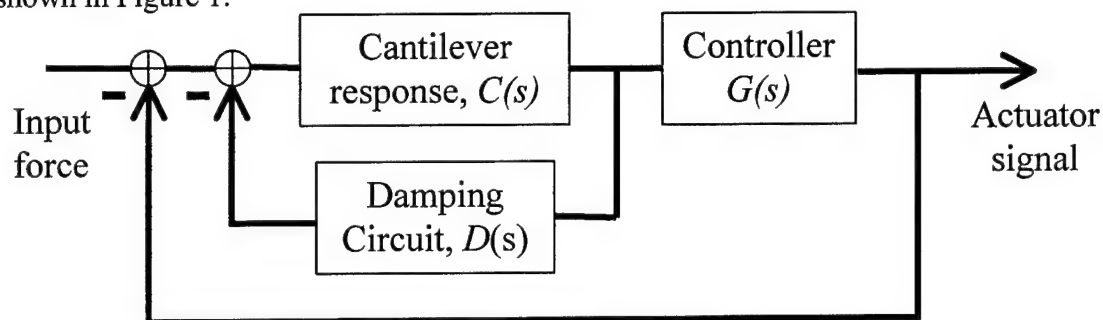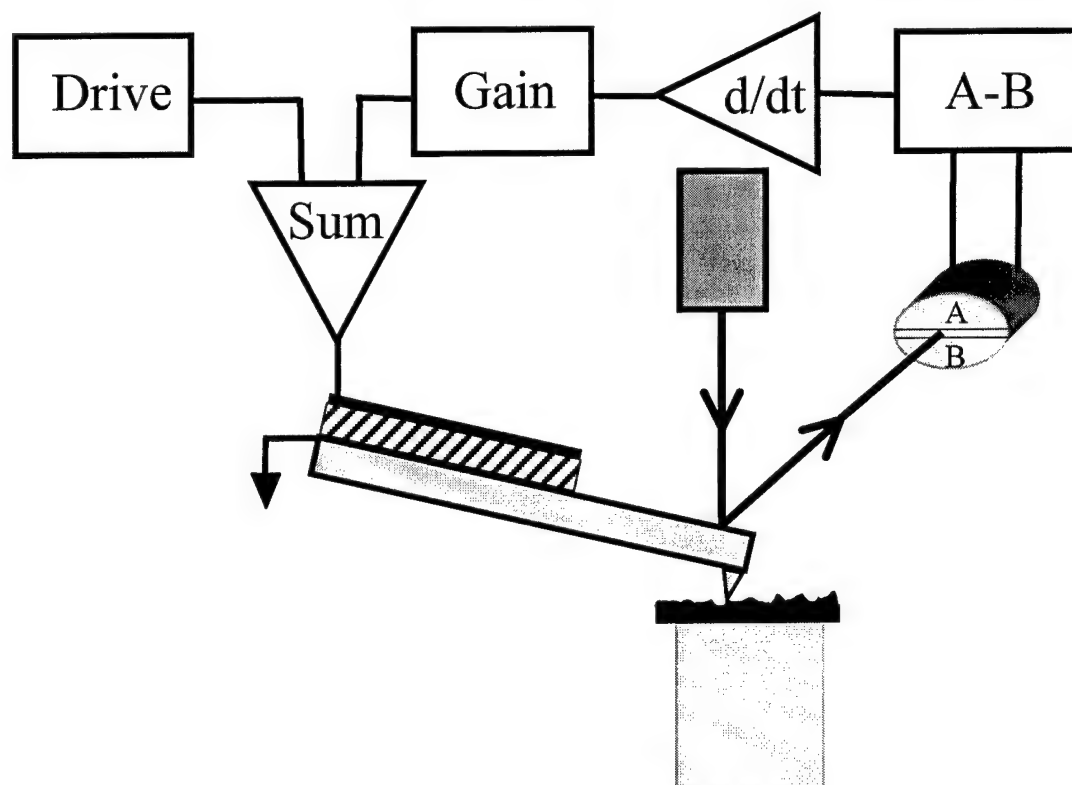

Figure 15   Block diagram for feedback with active damping.

The feedback loop is designed with so as to provide control of the dynamics of the cantilever, as governed by a second order equation of motion. To control the Q, we

implement a differentiator. This is shown in Figure 16.

Figure 16   Circuit for active control of the cantilever. For damping, the gain of the loop should be negative.

The net effect is to create an active drive that maintains a constant tapping amplitude. In the frequency domain, the feedback acts as a frequency dependent filter.

When negative feedback is used, the effect is a notch filter at the resonance, as shown in Figure 17, which gives a plot of the response of the cantilever and its drive. Figure 17a represents a simulation of the system described in Figure 17, while Figure 17b shows data.
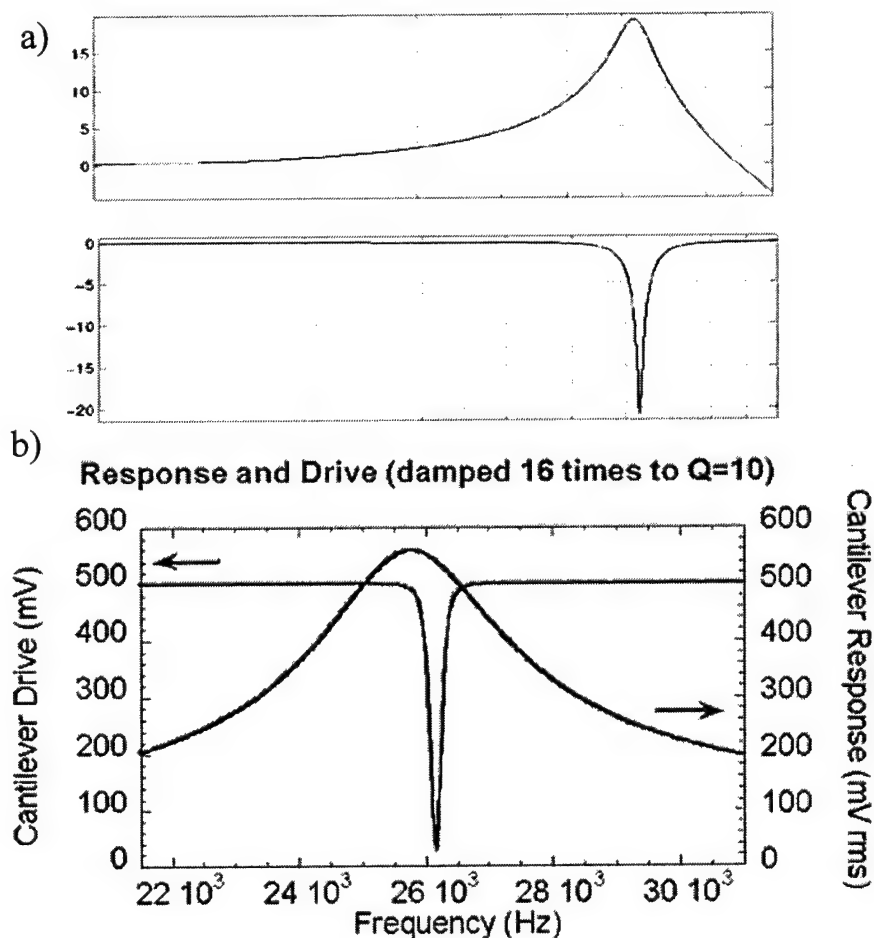

Figure 17   a) Simulated damped cantilever response and drive to produce the response. b) Damped cantilever response and the drive to produce the response.

The shift in the resonance is caused from phase lag in the electronics. This data was taken using an AD711 as the amplifier in the variable gain circuit. At 50 kHz, the phase lag for 1x gain is 3 degrees. However, for 10x gain, there is almost 20 degrees of phase lag.

The damping circuit is able to control the cantilever motion over a wide range via a variable gain stage. In Figure 5 we show the resonance of a cantilever with a natural Q of 260. The resonance can be reduced by adjusting the gain, down to an apparent Q value of 9, as measured by the resonance frequency divided by the width at half maximum energy. If the gain is reversed, the resonance response is increased up to value of several

thousand. An increased resonance increases the attractive regime for soft imaging in liquid environments or high resolution mass spectroscopy.[24]
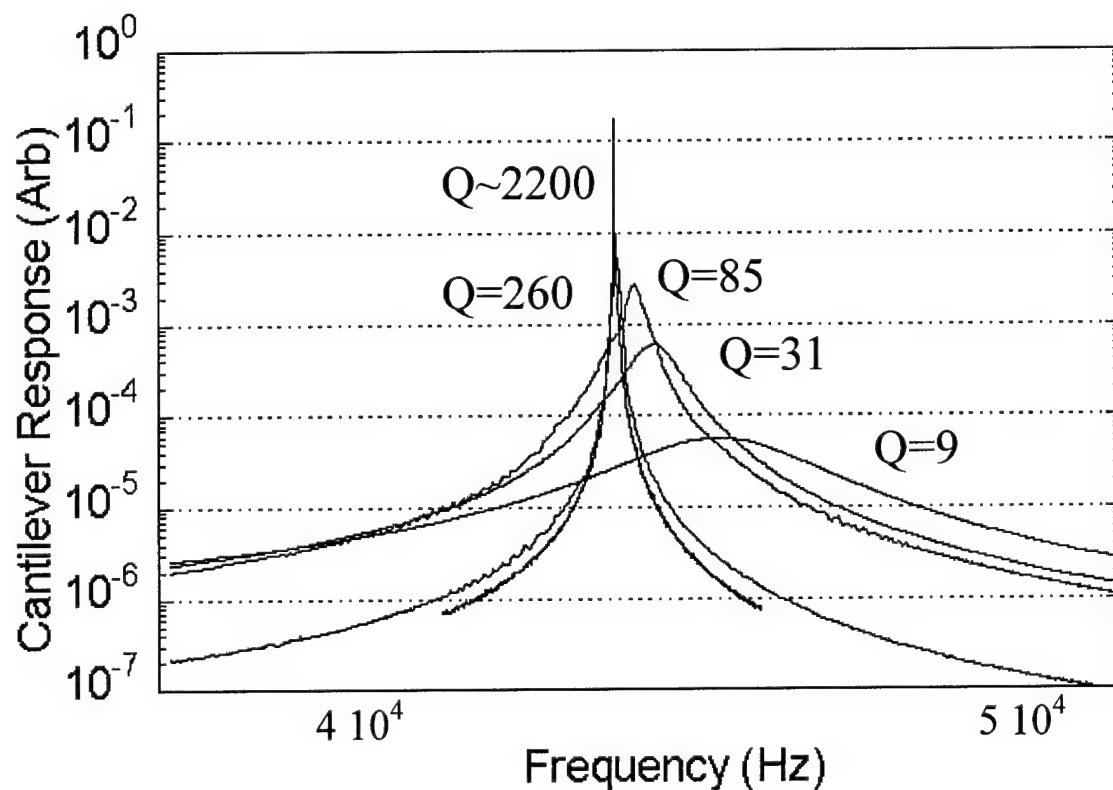

Figure 18   Control over the cantilever response demonstrated with effective Q values spanning over 3 orders of values.

In trace (a) in Figure 19, we again show the amplitude of a ZnO cantilever at resonance with a resonant frequency of 46 kHz and a Q of 150. In trace (b), we show the response is reduced by a factor of 10. The ZnO cantilever is uniquely suited for active damping when compared to the response of a typical cantilever driven by a piezoslab shown in trace (c).
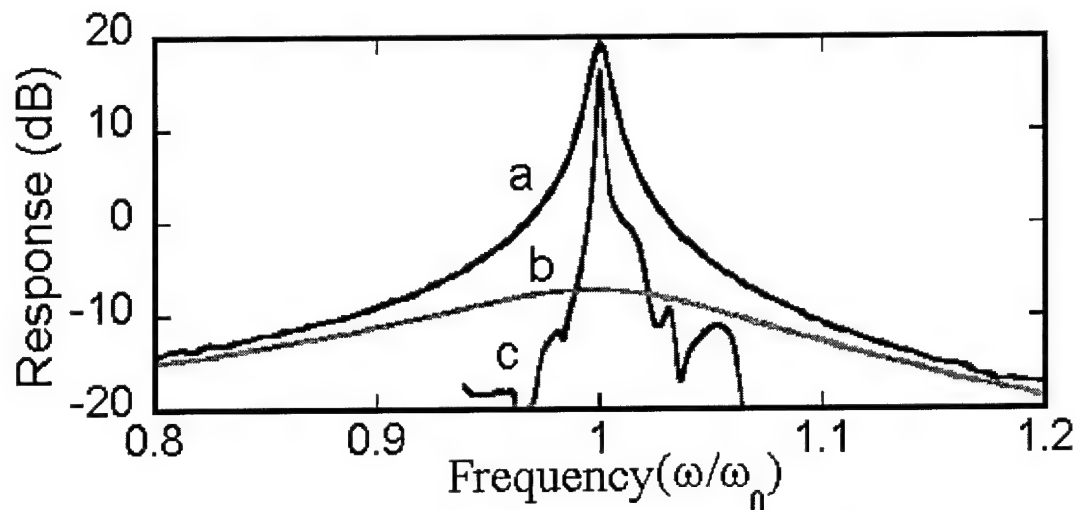
Figure 19   a) Native response (Q=150), b) actively damped response, and c)
             acoustically driven response.

In most AFMs, cantilevers are excited with a piezoslab located on a cantilever holder. The mechanical connection in this arrangement creates spurious responses for both amplitude and phase. These deviations from the ideal second order system make active control difficult to stabilize and maintain.

In Figure 20 we show the effect of active control on the cantilever ring-up time. Here we display the error signal versus time when the cantilever suddenly loses contact with the surface. These results were obtained by tapping on a bare silicon sample that was quickly retracted at $t = 0$.[25] In Figure 20b is the error signal for a cantilever with no active control. Reducing the response at resonance by a factor of two with active damping produces the faster ring up time shown in trace (a). We can also increase the response at resonance by reversing the gain of the active damping circuit. Trace (c) shows the slower response that results.
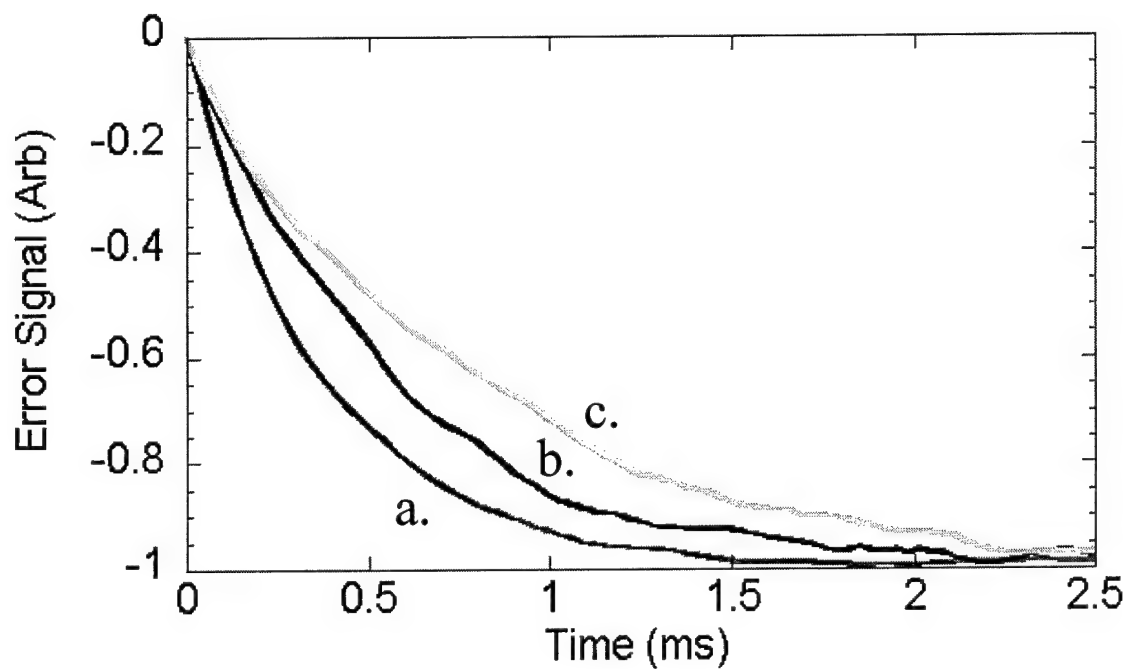
29

Figure 20   Error signal ring up for a. damped cantilever (effective Q=40), b. native cantilever (Q=68), and c. enhanced cantilever (effective Q=115).

High Speed Tapping Mode Imaging

To demonstrate the benefits of these techniques, a comparison between scans with the piezotube actuator (a) and the actively damped ZnO actuator (b) is shown in Figure 21.
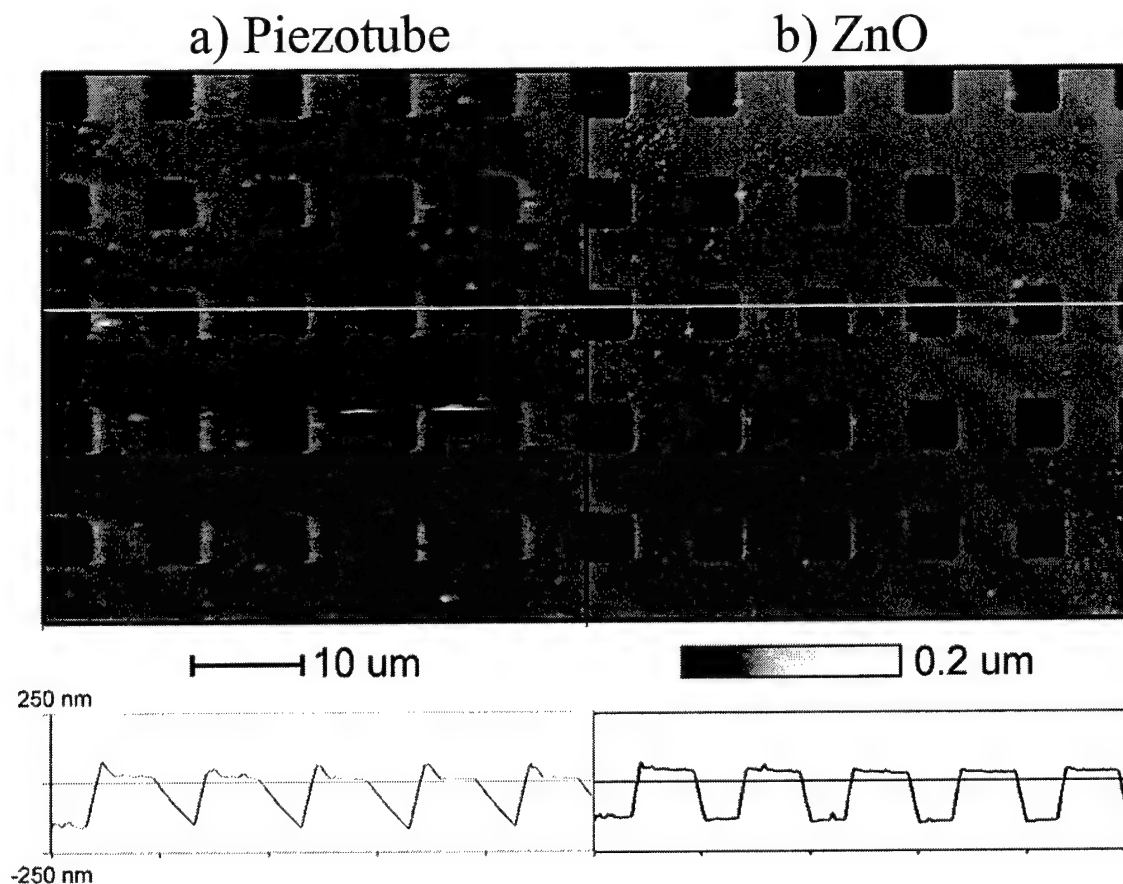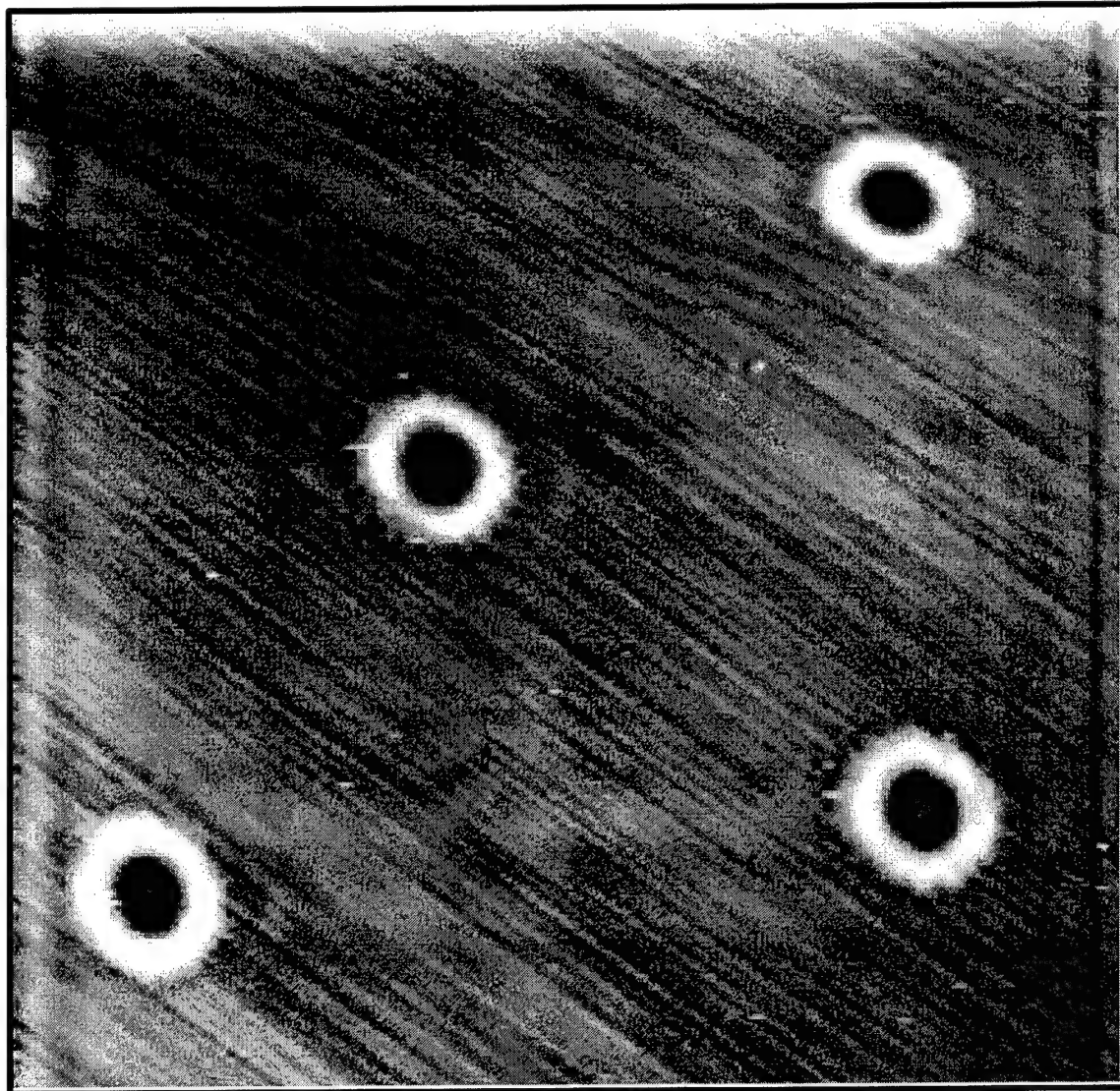
Figure 21   Image and line trace of a silicon grating with a) piezotube and b) damped ZnO actuator. In both cases the scan rate is 5 Hz.

A two-dimensional grating with 200 nm pits etched in silicon oxide are imaged with a traditional piezotube and the actively damped ZnO actuator. The square grating is a good test structure because the topography is unambiguous. Both images were taken with a scan rate of 5 Hz, with equal tapping amplitudes, setpoints, and optimized gains. A typical line trace is shown below each image. The image taken with the piezotube as the z-axis actuator does not follow the step closely, and tends to become unstable when changes in height are encountered. The sloped sidewalls in the line trace reveals that the rate is limited by the feedback. However, the scan with the actively damped ZnO cantilever faithfully reproduces the sample topography at the same scan speed.

The high speed capabilities are fully demonstrated with the image shown in Figure 22 of laser zone texturing on a hard drive disk.[26]

20 μm

Figure 22   Laser zone texturing on a hard drive disk taken with the damped ZnO. The scan is taken
                 at 15 Hz.

The semiconductor industry puts a large amount of effort into quality control of the texturing on hard drive disks because these features are critical to keep the read-write head from sticking to the disk as it powers down. AFMs are used to image every hard disk produced. This image is acquired 10 times faster with no loss of resolution. The polishing lines are clearly visible. This image was acquired at a scan rate of 2.4 mm/s which corresponds to a 256 x 256 pixel image in less than 16 seconds.

Improving Imaging Dynamics with Active Damping

For the images shown above, the actuator signal sent to the cantilever follows the topography of the sample. Scans over the grating, will therefore send signals approximating a square wave to the cantilever. This will have the effect of exciting the resonances of the cantilever. In Figure 23a. we demonstrate this by hitting the piezoelectric actuator with the square wave voltage pulse. This is what would happen if we encountered a step in topography. The feedback will apply a voltage to bend the cantilever over the step. As we do however, the resonance is immediately excited, just as if you ring a bell. With active feedback, we suppress the resonances so the tip more accurately tracks the desired input (Figure 23b).
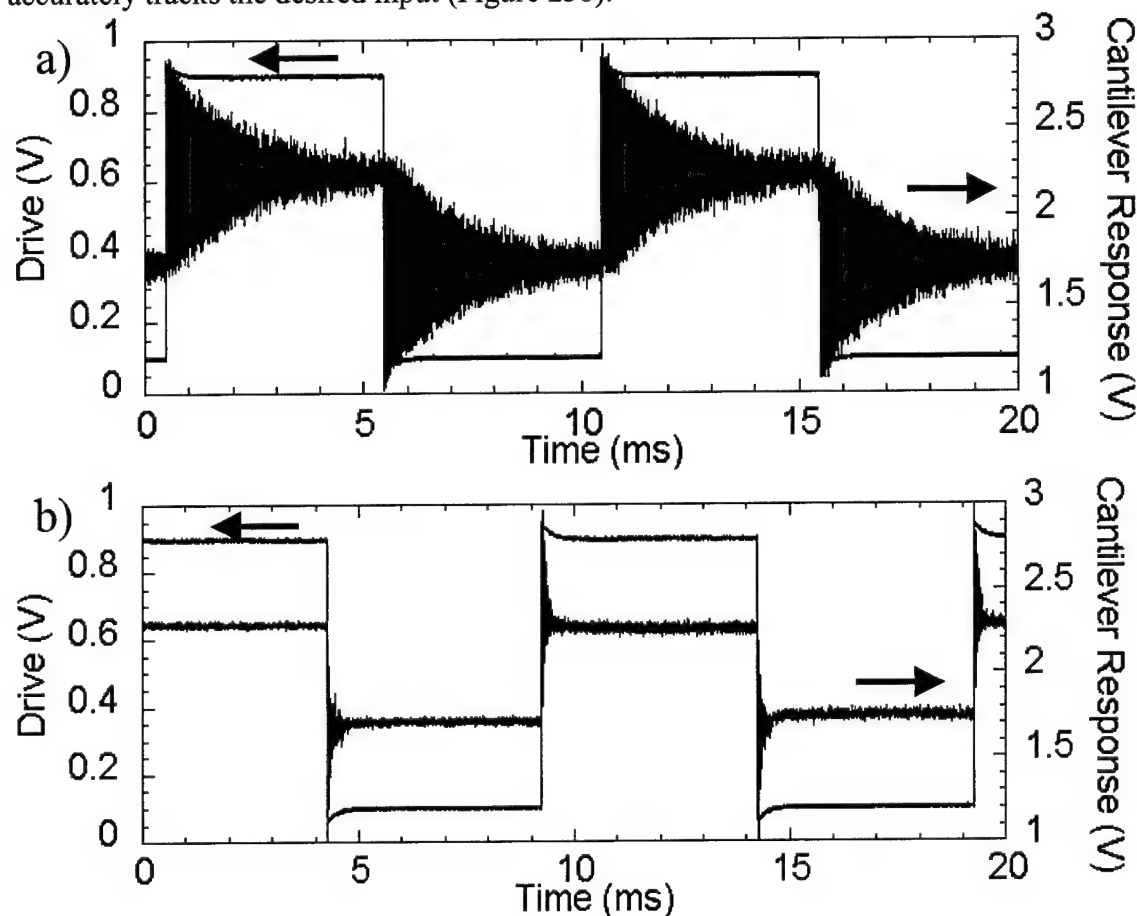

Figure 23   Cantilever response to square wave input for the a) native case and b) damped case.

As first shown in chapter 2 Figure 10, we obtain a 4 times improvement in speed due to the instrumentation—the speed increase is achieved through the active drive. A closer look at the actual signal driving the cantilever is shown in Figure 2410.
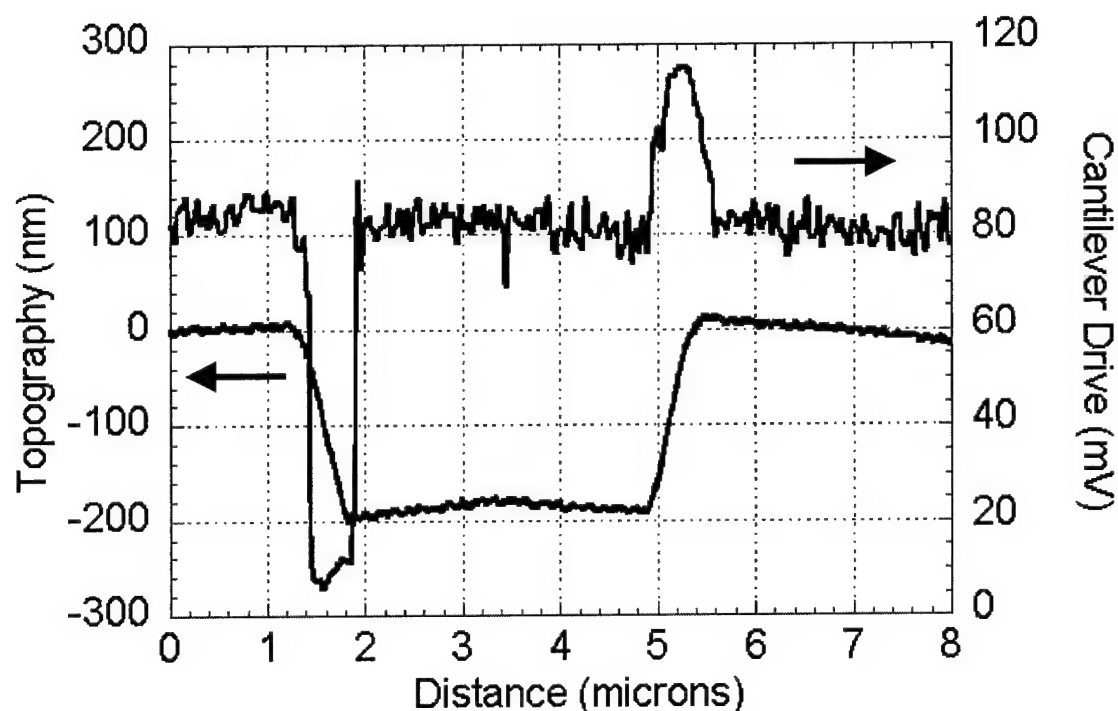
Figure 24   Active cantilever drive while scanning over pits etched in silicon oxide

Here, we are again scanning over a grating from left to right, but in addition to the topography signal we include the drive at the cantilever. The drive of the cantilever with the active control off is 80 mV. We see that the drive decreases as we scan over the step-down, but increases as the tip encounters a step-up. The effect of the decreased drive during the downward step is to limit the spurious increase in amplitudes due to contact with the surface. Conversely, when scanning over an upward step, spurious peaks are no longer a concern. Now, the concern is sticking between the tip and surface. The increased drive counteracts this tendency.

Soft Tapping Mode Imaging

A concern of the increased speed provided by the damping instrumentation is the increase in force between tip and sample. In order to gain insight into the relative forces involved while scanning in native mode, and scanning in damped mode at increased speed, we imaged a polymer gel sample specially designed to gain insight. The sample is composed of microlayers of polyethylene with alternating layers of high- and low-density polymers (0.92 g/cm^3 and 0.86 g/cm^3). The greater density polymer corresponds to a stiffer material. As the tip scans across the layers, the tip-sample force indents both layers, but with less indention for the stiffer material. Therefore, a measure of the scanning force can be obtained by comparing the relative heights of the layers. This technique has been described before.[27] A more accurate measure is obtained by monitoring the phase between the response and the drive. A phase increase indicates a loss of energy from the cantilever oscillation to the sample; phase is proportional to the energy loss per tap.[28] Therefore, by monitoring the phase during a scan, one has a metric by which to determine tapping force.

34

In Figure 25, we show topography of the polyethylene layers revealed by native scanning with the piezotube as the feedback actuator (a) and fast scanning with the damped ZnO cantilever (b). Even though the scan in (b) is over ten times the speed, the lower height difference between the layers suggest that the tapping force is reduced. We attribute this lower force to better feedback control resulting from increased feedback gain.
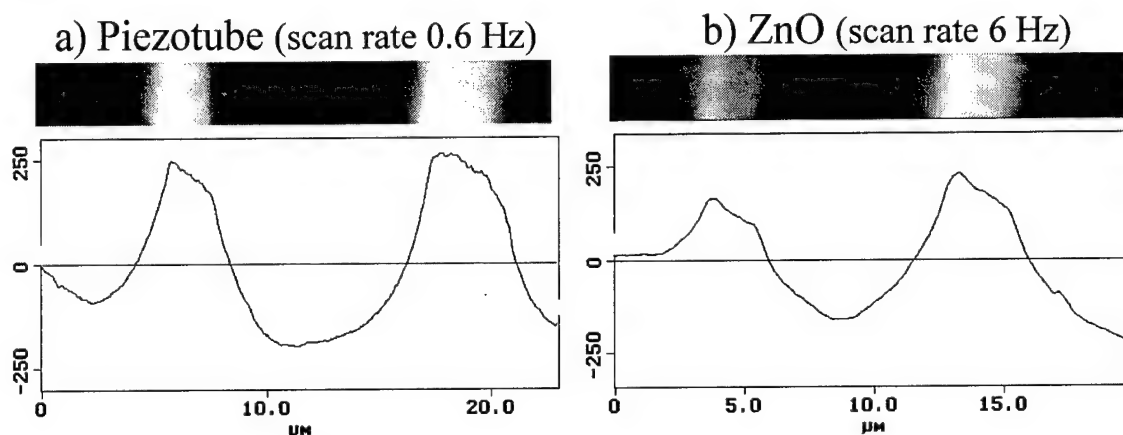

Figure 25   Comparison of the standard and fast scanning systems. The sample is a gel of alternating densities designed to indent under applied force. In part a) the piezotube is the feedback actuator, scanning at 0.6 Hz. In part b), the ZnO is the feedback actuator, scanning at 6 Hz.

In Figure 26, we examine the phase. Phase was measured while scanning, by monitoring the response of the cantilever (as measured from the photodiode) with the cantilever drive (measured as the output of the adder for the drive signal and damped circuit signal) as a reference. Topography is also shown. (a) shows the native scan with the piezotube actuator, taken at 0.6 Hz. The scan over the softer material produces a phase increase of approximately 4 degrees. In (b) we use the ZnO actuator with damping control. The scan in (b) shows a scan at 6 Hz, with no noticeable phase increase. The phase is again approximately 4 degrees over the area where the drive is in transition. This data indicates that forces between the tip and sample are reduced, even when scanning at a faster speed. The apparent lower bandwidth of the phase trace in the damped cantilever case is due to limits in the lock in amplifier when the cantilever scans at a higher velocity.
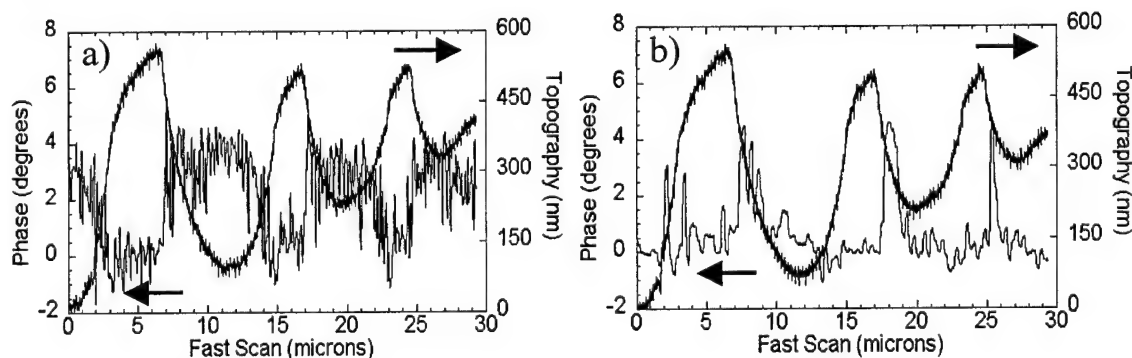
Figure 26   Comparison of the standard piezotube, part a), and fast ZnO, part b),
               scanning systems. Topography and phase imaging are shown in each.

The ramifications could have a profound effect on imaging of soft samples. Biological samples, such as DNA are easily damaged while imaging. Moreover, large tapping forces will distort soft samples, leading to an apparent increase in feature size. It is critical to maintain small force while imaging these samples. Yet it is also important to scan quickly. Currently, for soft imaging on delicate samples, many will resort to an imaging mode called "non-contact" mode where the scan is operated at a setpoint to obtain an effective attractive force when the tip and sample are in contact. Tapping mode operates in the repulsive regime such that the tip and sample repulse each other when in contact. The reason for this is to reduce the force between tip and sample. Scans designed to maintain non-contact mode must be done with careful attention to scan parameters and this normally necessitate a very slow scan. We have found that with proper instrumentation, a soft scan may be achieved while also gaining an increase in scan speed.

Figure 27   Images of DNA on mica (left) with error signal (right). In a), a piezotube scans the DNA with a scan rate of 5 Hz and an error signal of 30 mV. In b), a damped ZnO cantilever scans with a scan rate of 20 Hz and an error signal of 3 mV. In c), again with a 20 Hz scan rate, the DNA is shown to have a linewidth of under 11 nm.

To demonstrate this, we show in Figure 27a an image of DNA lambda phage (a virus that infects *E. coli*) taken with the traditional piezotube as feedback actuator. This

37

image was taken at 5 Hz and at this speed the error signal is quite large, with units of over 30 mV. This is a significant fraction of the total tapping amplitude. With the fast scanning techniques, we increase the speed to over 20 Hz, with a reduced error signal of under 3 mV (Figure 27b). The smaller error signal indicates a decreased vertical force on the sample, which is critical to maintain the structure of delicate samples. Most importantly, we suffer no loss in x-y resolution. The width of DNA is approximately 2 nm, but the convolution of the tip and the DNA prevents the resolving of the true width. If we zoom in slightly, we can again obtain an image at 20 Hz and measure the DNA width to be under 11 nm (Figure 27c). For an image in air, using standard silicon tips, this is among the best resolution shown, with the advantage of a decrease in imaging time by a factor of seven.

Conclusion

In Figure 28, we show a plot describing the capabilities of the AFM with a piezotube actuator versus the AFM with a ZnO actuator. On the vertical is amount of time to record a 256 x 256 pixel image in seconds. On the horizontal scale is the size of one side of the image, in microns and nanometers. Qualitatively, we expect larger images to take more time to image, as the tip is required to scan at faster speeds for the same scan rate.

Figure 28   Schematic showing plots of image size versus time required to acquire a
256x256 pixel image for tapping mode in air. The upper line corresponds
to times achievable with a piezotube actuator. The region above and to the
left of this line is accessible to the AFM. A corresponding line is shown
for the damped ZnO. Two points are added. Point a) shows typical time
scales for crystallization of polyethylene oxide on silicon (30 micron, 30s).
Point b) corresponds to the time for a single cantilever to compete with 92
well gel electrophoresis (1 micron, 40s).

Two typical imaging times for a given scan size with the piezotube system are
shown on the upper line. We plot two points. The first is a 90 second imaging time for

700 nm x 700 nm image of DNA. For a given error signal, the maximum scan rate was 2.7 Hz for this image. We also plot a 155 second image of an 80 μm x 80 μm section of a hard drive disk. The maximum scan rate for this image was just under 1.7 Hz. Above and to the left of this line corresponds to the regime that the piezotube system can faithfully access. For example, if we wanted to image a sample that was one micron on a side, we could expect this to take a little over 90 seconds. This time is a guideline since the true imaging time will depend on a host of parameters, including the viscous damping of the cantilever, surface topography, setpoint, tapping amplitude, sample stiffness (increases phase), resolution of the tip, and pixel size.

The second line describes typical imaging times for a given scan size in the ZnO system with active control. The two plotted images are described in this chapter. This system is able access all size and time combinations above this line.

We plot two points that can only be time resolved by the ZnO system. The crystallization of polyethylene oxide on silicon evolves with a time scale of approximately 30 seconds for a given temperature of interest.[29] In addition, we plot the time necessary for one image if a single cantilever is to compete with a 92-well gel electrophoresis. We assumed a 1 micron scan size and a one hour gel time. Therefore, every image should be taken every 40 seconds.

Estimates of Technical Feasibility

The research carried out under this contract provides a sound base for the commercialization of a very high speed atomic force microscope based on a MEMS cantilever with an integrated actuator and specialized circuitry. Typical microscopes scan at tens to hundreds of microns per second. We have demonstrated scan speeds of up to a centimeter per second. This speed advance changes the whole look and feel of the AFM from a research tool that takes hours of use to obtain final data, to a tool that images in real time with scan and zoom capabilities. This will both change the how the AFM is perceived for high throughput manufacturing applications as well as open new doors for short time scale research applications. This program has shown that the high speed AFM is technically feasible.

Future Plans

We plan to continue to advance the state of the art in high-speed atomic force microscopy through further cantilever, microscope, and electronic innovation. We are currently jointly manufacturing, with Digital Instruments of Santa Barbara, CA, the technology developed under this contract. This innovation has been well received by the market, and both companies plan to continue its development.

Contract Delivery Status

The deliverables for this contract are: 1) monthly status reports, 2) three (3) semi-annual technical reports, and 3) one (1) final technical report. This report is the final

report, and represents the last report due on this contract. All required reports have been submitted complete and on time.

Report Prepared By

Stephen C. Minne, Ph.D.
President
NanoDevices
5571 Ekwill Street
Santa Barbara, CA 93111
805-696-9002
805-696-9003 (fax)
with co-authorship to Todd Sulchek, Stanford University

Appendix I: Declaration of Technical Data Conformity

The contractor, NanoDevices Inc., hereby declares that, to the best of its knowledge and belief, the technical data delivered herewith under contract No. DAAH01-00-C-R218 is complete, accurate, and complies with all requirements of the contract,

Date: September 30, 2002

Stephen C. Minne, Ph.D.
President, NanoDevices Inc.

Appendix II: Distribution List

Commander   2 Copies
U.S. Army Aviation and Missile Command
ATTN: AMSAM-RD-WS-DP-SB
(Mr. Alexander H. Roach, Technical Monitor)
Bldg. 7804, Room 205
Redstone Arsenal, AL 35898-5248

Commander   1 Copy
U.S. Army Aviation and Missile Command
ATTN: AMSAM-RD-OB-R
Bldg. 4484, Room 204
Redstone Arsenal, AL 35898-5241

Commander   1 Copy
U.S. Army Aviation and Missile Command
ATTN: AMSAM-RD-WS
Bldg. 7804, Room 247
Redstone Arsenal, AL 35898-5248

Director   1 Copy
Defense Advanced Research Projects Agency
ATTN: MTO (Dr. Christie R. K. Marrian)
3701 North Fairfax Drive
Arlington, VA 22203-1714

Director   1 Copy
Defense Advanced Research Projects Agency
ATTN: CMO/SBIR
3701 North Fairfax Drive
Arlington, VA 22203-1714

Director   1 Copy
Defense Advanced Research Projects Agency
ATTN: SBIR/DARPA Library
3701 North Fairfax Drive
Arlington, VA 22203-1714

Defense Technical Information Center   2 Copies
ATTN: Acquisitions/DTIC-OCP, Rm-815
8725 John J. Kingman Rd., STE 0944
Ft. Belvoir, VA 22060-6218

[1] Gene F. Franklin, J. David Powell, Abbas Emami-Naeini. Feedback Control of Dynamic Systems. Addison-Wesley Publishing Company, New York, 1994, p. 343.

[2] The Q of an oscillating system is defined as 2π times the mean stored energy divided by the work per cycle.

[3] A. R. Hodges, K. M. Bussmann, J. H. Hoh, "Improved atomic force microscope cantilever performance by ion beam modification," Rev. Sci. Instrum. **72**, 3880 (2001).

[4] J. Mertz, O. Marti, and J. Mlynek, "Regulation of a microcantilever response by force feedback," Appl. Phys. Lett. **62**, 2344 (1993).

[5] D. Rugar, O. Zuger, S. Hoen, C. S. Yannoni, H. M. Vieth, and R. D. Kendrick, "Force detection of nuclear-magnetic-resonance," Science **264**, 1560 (1994).

[6] J. L. Garbini, K. J. Bruland, W. M. Dougherty, and J. A. Sidles, "Optimal control of force microscope cantilevers controller design," J. Appl. Phys. **80**, 1951 (1996).

[7] K. J. Bruland, J. L. Garbini, W. M. Dougherty, and J. A. Sidles, "Optimal control of ultrasoft cantilevers for force microscopy," J. Appl. Phys. **83**, 3972 (1998).

[8] Richard Feynman, The Feynman Lectures on Physics Vol. 1, p. 24-3 (1963).

[9] F. M. Serry, P. Veuzil, R. Vilasuso, and G. J. Maclay, in *Proceedings of the Second International Symposium on Microstructures and Microfabricated Systems*, Chicago (Electrochem. Soc., Pennington, NJ, 1995), p. 83.

[10] MATLAB UNIX & LINUX: version 6, Release 12, Mathworks, Inc., Natick, MA.

[11] See appendix A.

[12] B. Anczykowski, B. Gotsmann, H. Fuchs, J. P. Cleveland, V. B. Elings, "How to measure energy dissipation in dynamic mode atomic force microscopy," Appl. Surf. Sci. **140**, 376 (1999).

[13] Robert W. Stark, Tanja Drobek, and Wolfgang M. Heckl, "Tapping-mode atomic force microscopy and phase-imaging in higher eigenmodes," Appl. Phys. Lett. **74**, 3296 (1999).

[14] M. B. Viani, T. E. Schaffer, G. T. Paloczi, L. I. Pietrasanta, B. L. Smith, J. B. Thompson, M. Richter, M. Rief, H. E. Gaub, K. W. Plaxco, A. N. Cleland, H. G. Hansma, and P. K. Hansma, "Fast imaging and fast force spectroscopy of single biopolymers with a new atomic force microscope designed for small cantilevers," Rev. Sci. Instrum. **70**, 4300 (1999).

[15] H. J. Butt, P. Siedle, K. Seifert, K. Fendler, T. Seeger, E. Bamberg, A. L. Weisenhorn, K. Goldie, and A. Engel, "Scan speed limit in atomic force microscopy," J. Microscopy-Oxford **169**, 75 (1993).

[16] K. Wilder, C. F. Quate, B. Singh, D. F. Kyser, "Electron beam and scanning probe lithography: A comparison," J. Vac. Sci. Tech. B **16**, 3864 (1998).

[17] B. W. Chui, T. D. Stowe, T. W. Kenny, H. J. Mamin, B. D. Terris, D. Rugar, "Low-stiffness silicon cantilevers for thermal writing and piezoresistive readback with the atomic force microscope," Appl. Phys. Lett. **69**, 2767 (1996).

[18] S. S. Wong, E. Joselevich, A. T. Woolley, C. L. Cheung, C. M. Lieber, "Covalently functionalized nanotubes as nanometre-sized probes in chemistry and biology," Nature **394**, 52 (1998).

[19] J. H. Hoh, Y. Fang, T. Spisz, N. P. DCosta, R. H. Reeves, I. N. Bankman, "Solid state DNA sizing by atomic force microscopy," FASEB J. **11**, 1593 (1997).

[20] K.B. Mullis and F.A. Faloona, "Specific synthesis of DNA *in vitro* via a polymerase catalyzed chain reaction," Meth. Enzymol. **155**, 335-350 (1987).

[21] Y. Fang, T. S. Spisz, T. Wiltshire, N. P. DCosta, I. N. Bankman, R. H. Reeves, J. H. Hoh, "Solid-state DNA sizing by atomic force microscopy," Anal. Chem. **70**, 2123 (1998).

[22] A. T. Woolley, C. Guillemette, C. L. Cheung, D. E. Housman, C. M. Lieber, "Direct haplotyping of kilobase-size DNA using carbon nanotube probes," Nature Biotech. **18**, 760 (2000).

[23] Norio Ookubo and Seiji Yumoto, "Rapid surface topography using a tapping mode atomic force microscope," Appl. Phys. Lett. **74**, 2149 (1999).

[24] J. Tamayo, A. D. L. Humphris, A. M. Malloy, M. J. Miles, "Chemical sensors and biosensors in liquid environment based on microcantilevers with amplified quality factor," Ultramicroscopy **86**, 167 (2001).

[25] This exponential increase in error signal is also observed when imaging downward steps.

[26] R. Ranjan, D. N. Lambeth, M. Tromel, P. Goglia, and Y. Li, "Laser texturing for low-flying-height media," J. Appl. Phys. **69**, 5745 (1991).

[27] S. N. Magonov and D. H. Reneker, "Characterization of polymer surfaces with atomic force microscopy," Annual Rev. Materials Sci. **27**, 175 (1997).

[28] J. P. Cleveland, B. Anczykowski, A. E. Schmid, V. B. Elings, "Energy dissipation in tapping-mode atomic force microscopy," Appl. Phys. Lett. **72**, 2613 (1998).

[29] H. Schonherr, L. E. Bailey, C. W. Frank, "Analyzing the surface temperature depression in hot stage atomic force microscopy with unheated cantilevers: Application to the crystallization of poly(ethylene oxide)," Langmuir **18**, 490 (2002).